RECEIVED BY TIC JUL 16 1980

LBL-10883

CONF-800709--2

Lawrence Berkeley Laboratory

UNIVERSITY OF CALIFORNIA

MASTER

Invited lecture presented at the Seminar on High Energy Nuclear Interactions and Properties of Dense Nuclear Matter, Hakone, Japan, July 7-11, 1980

PION CONDENSATION AND INSTABILITIES: CURRENT THEORY AND EXPERIMENT

Miklos Gyulassy

May 1980

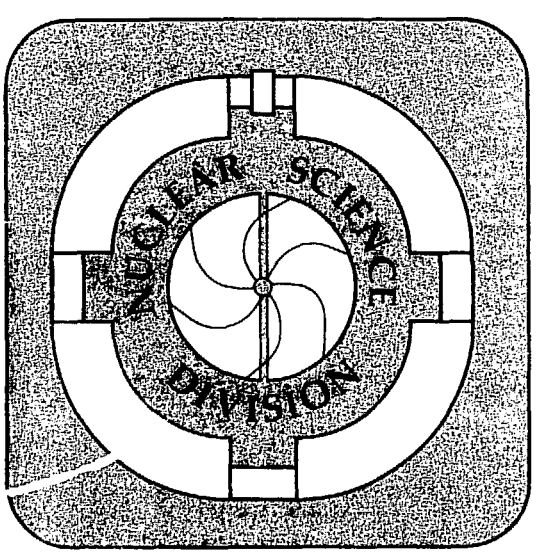

Prepared for the U.S. Department of Energy under Contract W-7405-ENG-48

DISTRIBUTION OF THIS DOCUMENT IS UNLIMITED

DISCLAIMER

This book was prepared as an account of work sponsored by an agency of the United States Government. Neither the United States Government nor any agency thereof, nor any of their employees, makes any warranty, express or implied, or assumes any legal liability or responsibility for the accuracy, completeness, or usefulness of any information, apparatus, product, or process disclosed, or represents that its use would not infringe privately owned rights. Reference herein to any specific commercial product, process, or service by trade name, trademark, manufacturer, or otherwise, does not necessarily constitute or imply its endorsement, recommendation, or favoring by the United States Government or any agency thereof. The views and opinions of authors expressed herein do not necessarily state or reflect those of the United States Government or any agency thereof.

PION CONDENSATION AND INSTABILITIES: CURRENT THEORY AND EXPERIMENT*

Miklos Gyulassy

Nuclear Science Division
Lawrence Berkeley Laboratory
University of California
Berkeley, California 94720

ABSTRACT

In this report we review current calculations of pion condensation phenomena in symmetric nuclear matter. The RPA and MFA methods are compared. Latest results[2] with a relativistic MFA theory constrained by bulk nuclear properties are then presented. The differences between equilibrium (condensation) and non-equilibrium (dynamic) instabilities are furthermore discussed. Finally, two-proton correlation experiments aimed at looking for critical scattering phenomena and two-pion correlation experiments aimed at looking for pion field coherence are analyzed.

---

*Invited lecture presented at the Seminar on High Energy Nuclear Interactions and Properties of Dense Nuclear Matter, Hakone, Japan, July 7 - 11, 1980.

DISTRIBUTION OF THIS DOCUMENT IS UNLIMITED

I. INTRODUCTION

In this report I will first discuss the status of current calculations of nuclear matter in the intermediate density range, $\rho_0 - 4\rho_0$, where $\rho_0 = 0.145\ fm^{-3}$, focusing on the topic of pion condensation. Second, I will discuss current and planned experiments using relativistic nuclear collisions to search for possible signatures of pion field coherence in this nuclear density range.

Since the mid 1970's, there has been much theoretical work[1] exploring the possibilities of new phases of nuclear matter at high densities. This work was stimulated in part by the need in astrophysics to know the equation of state of dense nuclear matter in calculating supernova explosions and properties of neutron stars, and in part by the new generation of nuclear accelerators that promised to create dense nuclear matter for the first time in the laboratory. Also, the sheer fun of speculation has motivated much work in this area. Had we a complete *solvable* theory of hadronic interactions, such speculations would of course be superfluous. However, for now we are obliged to speculate and extrapolate into the unknown density and temperature (ρ,T) domains using rather simplified approximation schemes. Progress in this field is then measured by the extent to which new "realistic" features are possible to incorporate into any given scheme. For example, the recent progress[2] discussed in Section II.C concerns our ability to incorporate the constraints imposed by the known bulk properties of normal nuclear matter in a self-consistent and covariant way into the theory of pion condensation.

In discussing different phases of nuclear matter we could start by specifying the expectation values of various nuclear current operators

$$J_\Gamma(x) = \langle\bar{\psi}(x)\Gamma\,\psi(x)\rangle \quad , \tag{1}$$

$$\Gamma = \{1, \gamma_5, \gamma_\mu, \gamma_\mu\gamma_5, \sigma_{\mu\nu}\} \otimes \{1,\underset{\sim}{\tau}\} \quad ,$$

where $\psi(x)$ is the nuclear field operator. (Non-relativistically only $\Gamma = \{1,\underset{\sim}{\sigma}\} \otimes \{1,\underset{\sim}{\tau}\}$ are distinct.) In the normal (symmetric) nuclear state, $J_\Gamma \neq 0$ only for $\Gamma = 1,\gamma_0$, both of which reduce non-relativistically to the nuclear density ρ. A state with $\underset{\sim}{J}_{\mu 5} = \langle\bar{\psi}\gamma_\mu\gamma_5\underset{\sim}{\tau}\psi\rangle \neq 0$ is, on the other hand, abnormal and corresponds to what we call the pion condensed phase. Our problem is to determine under what conditions are $J_\Gamma \neq 0$ for certain Γ.

Clearly, we first need to know the interactions in all possible spin and isospin channels. If QCD turns out to be the true theory, then these interactions would be described by the exchange of one, two, or more quarks between the nucleons as illustrated here.

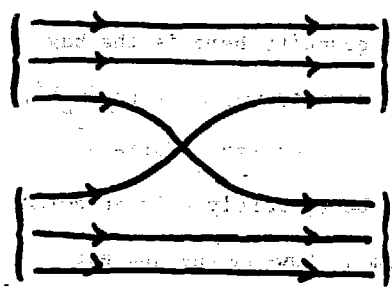

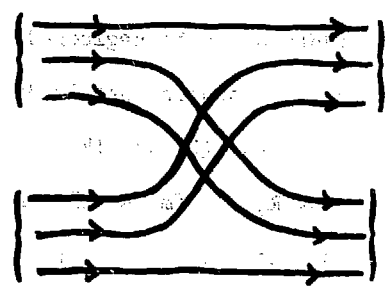

This van der Waals type of interaction would be non-local and involve the unknown large distance properties of QCD. Such forces are not calculable as yet. However, an effective description of these forces may be possible by introducing interpolating meson fields to represent these multiquark exchange processes in specific spin-isospin channels.

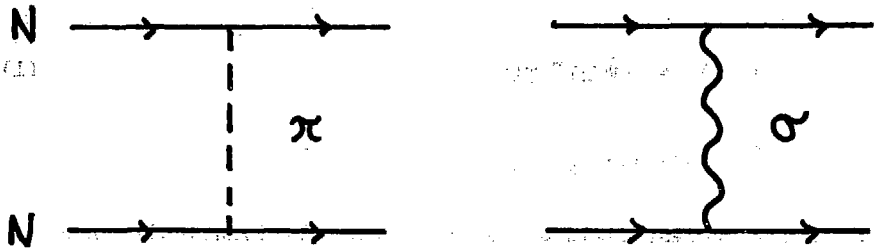

This is the historical approach to nucleon-nucleon interactions that we follow here. Thus, an array of meson fields $\sigma(J^{\pi} = 0^{+}, I=0)$, $\underset{\sim}{\pi}(0^{-},1)$, $\omega_{\mu}(1^{-},0)$, $\underset{\sim}{\rho}_{\mu}(1^{-},1)$, ... is introduced with standard Yukawa coupling

$$\mathcal{L}_{NN}^{int} = g_s \sigma \bar{\psi}\psi - g_\omega \omega_\mu \bar{\psi}\gamma^\mu\psi - \tfrac{1}{2} g_\rho \underset{\sim}{\rho} \bar{\psi}\gamma^\mu \underset{\sim}{\tau}\psi + f_\pi \partial_\mu \underset{\sim}{\pi}\, \bar{\psi}\gamma^\mu\gamma_5 \underset{\sim}{\tau}\psi + \ldots \tag{2}$$

It is clear that Eq. (2) can only be expected to provide a reasonable description of nuclear forces when the intrinsic quark structure of the hadrons can be neglected. The relevant quantity here is the bag radius R_B of a hadron that leads to a critical density $\rho_c/\rho_0 = (r_0/R_B)^3$, beyond which Eq. (2) is likely to break down. High energy theorists[3] insist that $R_B \approx 1$ fm, so that Eq. (2) may, at best, barely hold at normal nuclear density ($\rho_0 = 0.145$ fm^{-3}, $r_0 = 1.18$ fm). Low-energy nuclear theorists[4] have argued that $R_B \approx 0.3$ fm so that Eq. (2) may hold up to very high densities of $\sim 50\ \rho_0$. Not surprisingly, intermediate energy (π-nucleus) theorists[5] have argued that $R_B \approx 0.72$ fm, implying that Eq. (2) has some limited domain of applicability, perhaps up to $\sim 4\rho_0$. Needless to say, none of the above estimates is convincing. My prejudice leans toward the last estimate and thus toward the applicability of some

effective meson field theory in the intermediate density range, $\rho_0 \lesssim 4\rho_0$.

Having committed ourselves to a Lagrangian involving the interpolating meson fields, we are then confronted with the task of solving the following prototype coupled field equations

$$(i\partial\!\!\!/ - m + g_s\sigma - g_\omega \omega\!\!\!/ - g_\rho \underset{\sim}{\rho}\!\!\!/ \cdot \underset{\sim}{\tau}/2 + f_\pi \gamma_5 \partial\!\!\!/ \underset{\sim}{\pi} \cdot \underset{\sim}{\tau})\psi = 0 \quad , \tag{3a}$$

$$(\Box + m_\sigma^2)\sigma = g_s\bar{\psi}\psi - \partial U/\partial\sigma \quad , \tag{3b}$$

$$(\Box + m_\pi^2)\underset{\sim}{\pi} = - f_\pi \partial_\mu \bar{\psi} \gamma^\mu \gamma_5 \underset{\sim}{\tau}\psi \quad , \tag{3c}$$

$$\Box\omega_\mu - \partial_\mu\partial^\nu\omega_\nu + m_\omega^2\omega_\mu = g_\omega\bar{\psi}\gamma_\mu\psi \quad , \tag{3d}$$

$$\Box\underset{\sim}{\rho}_\mu - \partial_\mu\partial^\nu\underset{\sim}{\rho}_\mu + m_\rho^2\underset{\sim}{\rho}_\mu = g_\rho\{\tfrac{1}{2}\bar{\psi}\gamma_\mu\underset{\sim}{\tau}\psi + \underset{\sim}{\pi} \times \partial_\mu\underset{\sim}{\pi}\} \quad , \tag{3e}$$

in standard Bjorken and Drell notation. Although Eq. (3) is as yet intractable, it shows clearly that

$$\begin{aligned}
&\langle\bar{\psi}\psi\rangle \neq 0 && \Longleftrightarrow && \langle\sigma\rangle \neq 0 \quad , \\
&\langle\bar{\psi}\gamma_\mu\psi\rangle \neq 0 && \Longleftrightarrow && \langle\omega_\mu\rangle \neq 0 \quad , \\
&\langle\bar{\psi}\gamma_\mu\underset{\sim}{\tau}\psi\rangle \neq 0 && \Longleftrightarrow && \langle\underset{\sim}{\rho}_\mu\rangle \neq 0 \quad , \\
&\langle\bar{\psi}\gamma_\mu\gamma_5\underset{\sim}{\tau}\psi\rangle \neq 0 && \Longleftrightarrow && \langle\underset{\sim}{\pi}\rangle \neq 0 \quad ,
\end{aligned} \tag{4}$$

Therefore, instead of specifying the expectation value of the currents in Eq. (1), we can specify a given phase by the expectation values of the various meson field operators. These expectation values reflect the meson field configuration for a given nuclear state. In the normal symmetric nuclear state, $\langle\sigma\rangle \neq 0$, $\langle\omega_0\rangle \neq 0$, and all other field

expectations vanish. The point of displaying Eq. (3) is to emphasize the highly non-linear structure of these equations. Thus, it is quite possible that Eq. (3) can be satisfied by several distinct field configurations: $\{\sigma_i, \pi_i, \omega_i, \rho_i\}$.

The study of pion condensation involves finding the conditions under which $\langle \underset{\sim}{\pi}(x) \rangle \neq 0$ as a solution to Eq. (3). What differentiates the calculations in the literature[1] is the nature of the approximation scheme used to solve Eq. (3) and the choice of couplings within that scheme. Two main schemes have been used:[1] (1) Random Phase Approximation (RPA) and (2) Mean Field Approximation (MFA), although more sophisticated variational methods have also been used.[6] In the next section, methods (1) and (2) are reviewed and then our new results[2] with MFA are discussed.

II. THEORY OF PION CONDENSATION

A. RPA Method

This method, proposed by Migdal and refined by Weise and coworkers and many others,[1] searches for the pion condensation point by looking for Goldstone modes in the spin-isospin $(0^-,1)$ channel. A new phase involves the structural change of the ground state wavefunction breaking some symmetry such as parity or isospin. The Goldstone theorem asserts that when a symmetry is broken, then there must exist, in particular, a collective mode of the system with zero excitation energy. To calculate the collective modes in a particular (J^π, I) channel, we need, according to the Lehmann representation, only calculate the propagator $\Delta(\omega, \underset{\sim}{k})$ of the meson field with the same quantum numbers. In terms of the proper

self energy or polarization operator, $\Pi(\omega,k)$, of that meson with mass μ

$$\Delta(\omega,\underset{\sim}{k}) = [\omega^2 - k^2 - \mu^2 - \Pi(\omega,\underset{\sim}{k})]^{-1} \quad . \tag{5}$$

The spectrum $\omega(\underset{\sim}{k})$ of collective modes is then read off from the singularities of $\Delta(\omega,k)$ via

$$\Delta^{-1}(\omega(\underset{\sim}{k}),\underset{\sim}{k}) = 0 \quad . \tag{6}$$

Recalling that the propagator $i\Delta(x,y) = \langle T(\phi(x)\phi(y))\rangle$ measures the amplitude for field fluctuations, we see that when there exists a Goldstone mode $\omega(\underset{\sim}{k}) = 0$ for some $\underset{\sim}{k}$, then this means that it costs no energy to induce a field fluctuation of wavenumber $\underset{\sim}{k}$ in the medium. Since the meson field is always coupled to some current $\bar{\psi}\Gamma\psi$ as in Eq. (2) with the same quantum numbers, these spontaneous meson field fluctuations lead to spontaneous current fluctuations. Beyond the phase transition point, when Eq. (6) has solutions for complex $\omega(k) = \omega_0 \pm i\gamma_0$, then as shown for example in Ref. 7, these fluctuations grow exponentially in time, $e^{\gamma_0 t}$, until certain non-vanishing values of $\langle\phi\rangle \neq 0$ and $\langle\bar{\psi}\Gamma\psi\rangle \neq 0$ are reached. Of course, the calculation of the final $\langle\phi\rangle$ is beyond the RPA method and requires at least the MFA method.

To calculate the critical density of the phase transition, we must search for a value of the density that solves

$$k^2 + \mu^2 + \Pi(0,\underset{\sim}{k}) = 0 \quad . \tag{7}$$

In actual calculations of pion condensation,[1] Π is approximated by the pion self energy due to the strong p-wave πNN and $\pi N\Delta$ vertices, together with an effective short range interaction g' between particle-hole

pairs. This leads to the following structure of Π in symmetric nuclear matter.

$$\Pi = \frac{\Pi_N + \Pi_\Delta}{1 - g'\frac{1}{k^2}(\Pi_N + \Pi_\Delta)} \tag{8}$$

where Π_N is the nucleon particle-hole propagator (Lindhand function)

$$\Pi_N(0,\underset{\sim}{k}) \approx -f_\pi^2 k^2 F_{\pi N}^2(k)\ 2m^* p_F/\pi^2 \tag{9}$$

with $f_\pi \approx 1/m_\pi$, m^* is the effective nucleon mass, p_F is the Fermi momentum, and $F_{\pi N}$ is the πNN form factor. The Δ particle-nucleon hole propagator Π_Δ is given by

$$\Pi_\Delta(0,\underset{\sim}{k}) \approx -f_\Delta^2 k^2 F_{\pi\Delta}^2(k)\ \frac{1}{\omega_\Delta}\ \frac{p_F^3}{3\pi^2} \quad . \tag{10}$$

where $\omega_\Delta = 2.4\ m_\pi$, $f_\Delta^2 \approx 5/m_\pi^2$, and $F_{\pi\Delta}$ is the $\pi N\Delta$ form factor. Estimation for the value of g' varies between 0.5 ± 0.2 and is the subject of considerable theoretical controversy.

The functional forms of Π_N and Π_Δ are easily understood as follows: Both Π_N and Π_Δ describe the amplitude for the pion to create a virtual particle and hole excitation in the medium. Therefore, the structure of both self energies is the familiar perturbation form

$$\Pi_i(\omega,\underset{\sim}{k}) = \sum_{\underset{\sim}{q}} \frac{|\langle\pi|\mathcal{H}_{int}|ph\rangle|^2}{\omega + \omega_h(\underset{\sim}{q}) - \omega_p(\underset{\sim}{q}+\underset{\sim}{k})} \quad , \tag{11}$$

where $\omega_h(\underset{\sim}{q})$ is the energy of the initial nucleon (hole) of momentum $\underset{\sim}{q}$ that absorbs the pion with form momentum $(\omega,\underset{\sim}{k})$ and $\omega_p(\underset{\sim}{q}+\underset{\sim}{k})$ is the energy of the intermediate particle with momentum $\underset{\sim}{q}+\underset{\sim}{k}$. For Π_N the intermediate

particle is a nucleon so that $\omega_h - \omega_p = -\underset{\sim}{q} \cdot \underset{\sim}{k}/m^*$. For Π_Δ the intermediate particle is a Δ_{33} resonance, so that $\omega_h - \omega_p \approx \omega_\Delta \approx 2.4\, m_\pi$, almost independent of $\underset{\sim}{k}$ and $\underset{\sim}{q}$. Thus, the energy denominators for $\omega = 0$ are very different for Π_N and Π_Δ.

Because both πNN and $\pi N\Delta$ interactions are p-wave, the numerator $|\langle \mathcal{H}_{int} \rangle|^2 \propto k^2$. However, for nuclear intermediate states, Pauli principle blocks occupied states and $|\langle \pi | \mathcal{H}_{int} | N\bar{N} \rangle|^2 \propto k^2\, n(\underset{\sim}{q})(1 - n(\underset{\sim}{k}+\underset{\sim}{q}))$, while no Pauli blocking occurs for Δ and $|\langle \pi | \mathcal{H}_{int} | \Delta\bar{N} \rangle|^2 \propto k^2\, n(\underset{\sim}{q})$. Here $n(\underset{\sim}{q})$ is the Fermi distribution of occupied states. Because Π_Δ does not involve Pauli blocking and the energy denominator is insensitive to $\underset{\sim}{q}$, we can simply sum over $\underset{\sim}{q}$ giving $\Pi_\Delta \propto k^2 \rho/\omega_\Delta$ as in Eq. (10). On the other hand, Pauli blocking severely limits the sum over $\underset{\sim}{q}$ for Π_N. As $k \to 0$ only those momenta $\underset{\sim}{q}$ inside the Fermi sphere that lie within a half shell of radius p_F and thickness k and oriented such that $\underset{\sim}{q} \cdot \underset{\sim}{k} > 0$ satisfy $n(\underset{\sim}{q})(1 - n(\underset{\sim}{q}+\underset{\sim}{k})) \neq 0$. The number of states in that shell is $\propto p_F^2 k$. The particle-hole energy denominator is then $\propto p_F k/m^*$, so finally we obtain $\Pi_N \propto k^2 m^* p_F$ as in Eq. (9). Even for $k \sim p_F$, this form for Π_N holds because then $\omega_p - \omega_k \propto p_F^2/m^*$, while the sum over $\underset{\sim}{q}$ gives p_F^3 in the numerator. Therefore, we see that the forms of Π_N and Π_Δ in Eqs. (9) and (10) are easily understood.

With Π given by Eq. (8), a typical Feynman many-body diagram that has been summed via Dyson's equation in Eq. (5) is

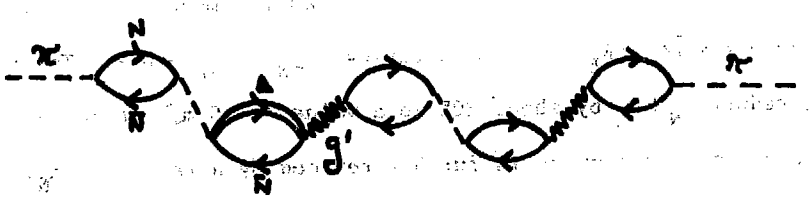

(12)

From such graphical analysis, it is clear that ($\omega \approx 0$, $\underset{\sim}{k} \approx 2m_\pi$) "pion" modes are basically coherent many-particle, many-hole excitations of the ground state wavefunction. These pions have very little to do with the familiar laboratory pions $\omega = \sqrt{k^2 + m_\pi^2}$. Although this point is obvious to most workers in the field, there is often much confusion about expectations of copious pion production associated with pion condensation. Pion condensation simply reflects a long-range correlation between the spin-isospin components of the nuclear wavefunction. It certainly does not imply that there are hundreds of real pions in the nucleus.

To get a feeling for the magnitude of the self energies involved in Eqs. (8-10), consider Π_N, Π_Δ and Π for $\rho = \rho_0$, $p_F \approx 1.8\ m_\pi$, $g' = 0.5$, $m^* = m_N$, and for pion momentum $k \approx 2m_\pi$. Setting $F_{\pi N} = F_{\pi\Delta} = 1$, we find $\Pi_N(0,2m_\pi) \approx -10\ m_\pi^2$ and $\Pi_\Delta \approx -2m_\pi^2$. Thus, the numerator of Eq. (8) is $\approx -12\ m_\pi^2$, while the denominator is ≈ 2.5, so that $\Pi(0,2m_\pi) \approx -5\ m_\pi^2$. Thus, we see that Π is large and cancels the kinetic energy $k^2 + m_\pi^2 = 5\,m_\pi^2$ at about normal densities.

Now consider the effect of finite form factors. Conventionally, $F_{\pi N}(k) = F_{\pi\Delta}(k) = (\Lambda^2 - m_\pi^2)/(\Lambda^2 + k^2) \approx 1 - (k^2 + m_\pi^2)/\Lambda^2$ is described by a monopole form factor with $\Lambda \approx 1$ GeV. Note, however, that this large value of Λ does not require an assumption that the quark bags are small. In Ref. (5), the form factor for the intermediate quark bag of radius $R_B = 0.72$ fm was computed as $F_{\pi N}(k) = F_{\pi\Delta}(k) = 3j_1(kR_B)/kR_B \approx 1 - (kR_B)^2/10$. For $k = 2m_\pi$, this in fact yields the same result as the monopole form factor with the large $\Lambda = \sqrt{12.5}/R_B = 970$ MeV, giving $F_{\pi N} = F_{\pi\Delta} \approx 0.9$. The net effect is to reduce $\Pi_N + \Pi_\Delta$ by about 20% to a value $\approx -10\ m_\pi^2$ at normal density. For $m^* < m_N$, this value is further reduced by a factor m^*/m_N.

We can conveniently summarize the combined influence of Π_Δ, g', and $F_{\pi N}$ on the self energy, Π, in Eq. (8) by defining an effective πNN coupling constant via

$$\Pi \equiv \left(\frac{f_{eff}}{f_\pi}\right)^2 \Pi_N = -f_{eff}^2\, k^2\, 2m^*\, p_F/\pi^2 \quad . \tag{13}$$

Comparing it with Eqs. (8-10), this effective coupling constant is given by

$$f_{eff}^2(k,p_F) = f_\pi^2 \frac{|F_{\pi N}(k)|^2 \left[1 + \frac{1}{6}\frac{f_\Delta^2}{f_\pi^2}\frac{p_F^2}{m^*\omega_\Delta}\right]}{1 + g'|F_{\pi N}(k)|^2 f_\pi^2 \frac{2m^*}{\pi^2} p_F \left[1 + \frac{1}{6}\frac{f_\Delta^2}{f_\pi^2}\frac{p_F^2}{m^*\omega_\Delta}\right]} \quad . \tag{14}$$

Although the form of this "constant" certainly does not look constant as a function of p_F, Table 1 shows that f_{eff}^2 is actually very insensitive to m^* and $\rho = 2p_F^3/3\pi^2$. The remarkable property of Eq. (14) is that in the density range ρ_0 to $3\rho_0$, where we expect m^* to vary between $(1.0 \sim 0.7)m_N$, f_{eff}^2 varies only by ~10%.

TABLE 1. Effective πNN coupling f_{eff} in units of fm for $k = 2m_\pi$, $g' = 0.5$, $|F_{\pi N}(k)|^2 = 0.81$ incorporating correlations, Δ production and form factors as a function of m^* and density from Eq. (14). Compare f_{eff} to $f_\pi = 1.41$ fm in free space.

m^*/m_N	ρ =	ρ_0	$2\rho_0$	$3\rho_0$
1.0	f_{eff} =	0.93	0.89	0.86
0.75		1.01	0.98	0.96
0.50		1.14	1.12	1.11

We note that the idea of using an effective coupling to incorporate Δ and correlation effects was first pointed out in Ref. (8) in connection with neutron matter. Similarly, we will exploit the near density independent of f_{eff} for symmetric matter to simplify mean field calculations in Section II.C.

A last point we wish to stress in connection with the pion self energy is the near proportionality of Π to the effective nucleon mass, $m^*(p_F)$. This means that the driving force for condensation depends sensitively on the details of the single particle-hole excitation spectrum and hence on nuclear structure physics. Therefore, pion condensation calculations should only be carried out with models consistent with known nuclear properties. An example of a model not consistent with nuclear properties is the usual chiral model[13] where $m^* = m_N$. Since $m^* < m_N$, the chiral model can be expected to overestimate $\langle \underset{\sim}{\pi}(x) \rangle$.

Thus far, we have discussed the pion self energy in cold ($T = 0$) nuclear matter at high densities. Since we are interested in whether π condensation can occur in relativistic nuclear collisions, we need to know also the effect finite $T \sim 50 - 100$ MeV has on the condensation.

In Section III we will consider non-equilibrium effects on condensation as well.

At finite T, the pion self energy still has the same structure as Eq. (11), but now the sum over occupied states involves the Fermi-Dirac distribution rather than a step function up to p_F. Since $\Pi(x,y)$ measures the correlation function for spin-isospin density fluctuations between points x and y, it is physically clear that at high T such correlations must wash out. Hence, finite T suppresses the pion self energy. We can define a critical temperature, $T_c(\rho)$, analogous to the Curie temperature in ferromagnets, such that $\langle \underset{\sim}{\pi}(x) \rangle \neq 0$ only for $T < T_c(\rho)$. In Fig. 1 we reproduce a figure prepared by Gudima and Toneev[11] comparing two calculations[10,12] of $T_c(\rho)$. In addition, Fig. 1 shows the dynamical trajectory of T vs. ρ calculated via the intranuclear cascade code of Ref. 11.

The difference between calculations RGG[10] and G[12] lies in the choice of form factors and g' and reflects typical theoretical uncertainties in the calculation of $T_c(\rho)$. The other curves in Fig. 1 show the calculated path of temperatures and densities followed in the reaction Ar + Ca at 0.5 GeV/A and Ne + U at 2.1 GeV/A. These curves illustrate that high enough densities together with low enough temperatures can be obtained for pion condensation to occur via relativistic nuclear collisions. However, the time spent in the π condensation region is only $t^* \sim (3\text{-}16)$ fm/c depending on the particle $T_c(\rho)$ curve. As shown in Fig. 7 of Ref. 7, the time required to create one $\pi^+\pi^-$ or $\pi^0\pi^0$ condensate ($\omega = 0$) pair with momenta $\underset{\sim}{k}$ and $-\underset{\sim}{k}$ is $t_c \sim 3$ fm/c. Therefore, we cannot expect a fully developed π condensate to form in such nuclear collisions. However, we can expect

the spin-isospin fluctuations associated with π condensation to increase significantly (see Eq. (56)) during the interaction time. As we discuss in Section III it may be possible to search for evidence of these increased fluctuations by looking for critical scattering phenomenon.

Although it is unlikely that the pion field reaches its final expectation value $\langle \underset{\sim}{\pi}(x) \rangle$ in a nuclear collision, it is interesting to compute what the maximum amplitude of the pion field $\langle \underset{\sim}{\pi} \rangle$ would be. In the next section we review the mean field theory methods for calculating $\langle \underset{\sim}{\pi} \rangle$

B. MFA Method

For the problem of π condensation, this method was first used by Sawyer, Scalapino, Baym, Campbell, Dashen, Manassah, and others.[1] For symmetric nuclear matter, MFA was used recently in Ref. 13. In Section II.C the most recent application[2] of MFA for symmetric nuclear matter will be described.

MFA is completely equivalent to the Hartree approximation. The ground state wavefunction $|\phi_0\rangle$ is assumed to be a single Slater determinant composed of quasi-particle wavefunctions satisfying Eq. (3a) with all meson field operators replaced by their expectation values: $\{\sigma, V_\mu, \underset{\sim}{\pi}, \ldots\} \rightarrow \{\langle\sigma\rangle, \langle V_\mu\rangle, \langle \underset{\sim}{\pi}\rangle, \ldots\}$. These expectation values are computed in turn from Eqs. (3b - ...), by replacing the current operators on the right-hand side by their expectation values as determined by $|\phi_0\rangle$. Since $|\phi_0\rangle$ is a function of the mean fields itself, the $\langle\phi_0|\psi\Gamma\psi|\phi_0\rangle$ are functions of $\{\langle\sigma\rangle, \langle V_\mu\rangle, \ldots\}$. Therefore, Eqs (3b - ...) reduce to a transcendental set of equations for determining the self-consistent

field configurations.

In MFA, two-, three-, etc. particle correlations are neglected. Why can we hope to get away with such a crude approximation? Correlations lead to a finite probability ε for finding a given nucleon in a state other than single-particle orbitals occupied in $|\phi_0\rangle$. This leads to Bethe's familiar observation that the overlap of $|\phi_0\rangle$ with the true ground state wavefunction in $\langle\psi_0\rangle$ is $\langle\phi_0|\psi_0\rangle \sim (1-\varepsilon)^A \sim e^{-\varepsilon A} \ll 1$ for many-body systems. Therefore, $|\phi_0\rangle$ is always a very very crude approximation to $|\psi_0\rangle$. Nevertheless, if we are interested only in the expectation values of few-body operators, then $|\phi_0\rangle$ may be adequate. For example, consider a one-body operator, $A = \sum a_i b_i^\dagger b_i$. Since $\langle\psi_0|b_i^\dagger b_i|\psi_0\rangle \approx \theta(E_F-\omega_i)(1-\varepsilon_i) + \theta(\omega_i - E_F)\varepsilon_i$, while $\langle\phi_0|b_i^\dagger b_i|\phi_0\rangle = \theta(E_F-\omega_i)$, $\langle\psi_0|A|\psi_0\rangle \approx (1-\langle\varepsilon\rangle)\langle\phi_0|A|\phi_0\rangle + O(\varepsilon)$. Similarly the error made in evaluating m-body operators using $|\phi_0\rangle$ is $O(m\varepsilon)$. This probability, ε, for exciting a particle out of a given orbital, is roughly $\varepsilon \approx V_{corr}\rho$, where V_{corr} is the correlation volume in which the interactions are so strong that excitations out of the Fermi sea are possible. Typically, $V_{corr} \approx 4\pi r_{corr}^3/3$ where $r_{corr} \sim 0.5-0.7$ fm. Since $\rho \approx (4\pi r_0^3/3)^{-1}$, $r_0 \approx 1.18$ fm, we estimate $\varepsilon \sim 0.1-0.2$. The Pauli principle helps keep V_{corr} so small. This is, of course, why the naive shell model of nuclear structure has been so successful for the past 40 years, and why Hartree-Fock and time-dependent Hartree-Fock methods have been able to provide much useful insight into nuclear structure and reactions.

We can see though that MFA becomes less reliable as the density increases. By $4\rho_0$, the MFA results are thus subject to considerable uncertainties. In using MFA to extrapolate to the intermediate density

region, this increasing uncertainty must always be kept in mind.

To help overcome part of the deficiency in this method, the coupling constants can be replaced by effective ones to simulate the effect of correlation and other higher order effects. For example, we saw in Eq. Eq. (8) that correlations via the g' parameter result in significant (~50%) quenching of spin-isospin density fluctuations. However, this quenching could be taken into account by a nearly density-independent renormalization of the πNN coupling constant via Eqs. (13) and (14). Therefore, if we replace the free space πNN coupling $f_\pi = 1/m_\pi$ in Eq. (2) by f_{eff} given by Eq. (14), then the main effect of correlation as well as Δ production and form factors can be taken into account. This is the procedure we will adopt in Section II.C.

It is important to emphasize that all parameters in the Lagrangian Eq. (2) when used in the mean field approximation are then *effective* coupling constants. Most of these effective coupling constants can be determined from the bulk properties of nuclear matter. This is how g_s, g_ω, and g_ρ are determine in Walecka's[4] mean field calculation and how Skyrme force parameters are determined in usual HF and TDHF calculations. Having determined the g_i this way, it makes no sense to sum higher order diagrams since their contributions are implicitly built into the values of g_i. As shown by Chin,[15] while the g_i which lead to consistent bulk nuclear properties are sensitive functions of the particular class of diagrams incorporated into the effective theory, the density dependence of the equation of state, $E/A(\rho)$, is not. The reason for this is that the higher order diagrams are only slowly varying functions of the density.[15] Thus the density dependence of the equation of state is mostly determined

by the mean field diagrams although the absolute scale is sensitive to all diagrams.

This situation should be contrasted to the traditional nuclear physics approach, where the parameters of the Lagrangian are chosen to reproduce the free space NN cross sections. In that case, correlations are incorporated by including new classes of diagrams via Breuckner or e^s theory. Except for the questionable non-relativistic approximation made, these approaches are then more fundamental than the MFA. However, they are rather unwieldy and complicated, especially when asked to calculate high (ρ,T) properties. It is here that the MFA has a clear edge in providing essentially analytical insight into the physics of high (ρ,T) nuclear matter.

Up to now, the discussion of MFA was in the context of an approximation scheme capable of calculating the equation of state, $E/A(\rho,T)$, as a function of ρ and T. In the context of normal nuclear matter, this approach has been actively pursued by Walecka and coworkers.[14,15] In the context of pion condensed matter, only recently has this approach been carried out in a complete form. These results are discussed in Section II.C. The large body of previous work[1] on MFA for π condensation involves a hybrid version of the MFA upon which we now elaborate.

In these hybrid MFA, no attempt is made to provide a consistent treatment of both normal and abnormal nuclear matter. Rather, the normal nuclear equation of state is assumed to be given. The effective Lagrangian is then not constrained by the bulk properties of nuclear matter but rather by certain fundamental properties of hadronic interactions. In connection with pion interactions, the most fundamental property is assumed to be

PCAC.[1] To incorporate PCAC, the chiral $(\sigma,\underset{\sim}{\pi})$ model of the Lagrangian $\mathcal{L}_{chiral}$ is then used as the starting point. With $\mathcal{L}_{chiral}$ the mean field approximation is made replacing the $(\sigma,\underset{\sim}{\pi})$ chiral pair fields by their expectation values $(\bar{\sigma}(x),\bar{\underset{\sim}{\pi}}(x))$. These expectation values are, however, constrained such that[13]

$$m^{*2} = g^2\{|\bar{\sigma}(x)|^2 + |\bar{\underset{\sim}{\pi}}(x)|^2\} = m_N^2 \quad , \tag{14a}$$

$$\tan\theta_{ch} = \frac{|\pi(0)|}{|\sigma(0)|} \quad , \tag{14b}$$

so that

$$\begin{aligned} g\sigma(x) &= m_N \cos\theta_{ch} \quad , \\ g\pi_{\pm}(x) &= m_N \sin\theta_{ch} \frac{e^{\pm ikx}}{\sqrt{2}} \quad . \end{aligned} \tag{15}$$

Here θ_{ch} is the chiral angle. In the normal state $\theta_{ch} = 0$. In a π condensed state, $\theta_{ch} > 0$. The mean field equations are then solved in the non-relativistic approximation, obtaining finally the equation of state: $E/A(\rho,\theta_{ch})$. However, as shown by Kerman and Miller,[16] $E/A(\rho,0)$ has no resemblance to the normal nuclear equation of state and does not even saturate. This is not surprising since there was no attempt to fix $\mathcal{L}$ from bulk nuclear properties and $\mathcal{L}_{chiral}$ does not provide a complete description of nuclear forces. To remedy this inherent difficulty, the following procedure is adopted to compute a condensation energy

$$(E/A)_{cond} = E/A(\rho,\theta_{ch}) - E/A(\rho,0) \quad . \tag{16}$$

It is hoped that the inherent inaccuracies associated with the normal nuclear state are thereby cancelled in the difference.

For symmetric nuclear matter we saw that the "driving force" toward condensation was $\Pi(\omega=0,\underset{\sim}{k}) \propto m^*$ and is therefore sensitive to the particle-hole specturm. Thus, the hope that Eq. (16) cancels the inaccurate treatment of the nuclear structure effects is not well founded when m^* is constrained to be m_N. Therefore, the driving force in this approach is (m_N/m^*) larger than in an approach where m^* is calculated dynamically.[2] Typically, $m^* \sim 0.9 - 0.7$ in self-consistent treatments. We can therefore expect this hybrid MFA approach to *over-estimate* both the condensation energy and $\langle\underset{\sim}{\pi}\rangle$. As we shall see below, this does indeed turn out to be the case.

C. π Condensation Consistent with Bulk Nuclear Properties[2]

To incorporate the constraints due to bulk nuclear properties in a self-consistent way, our starting point is the Walecka model.[14] We also incorporate non-linear scalar field interactions as did Boguta and Bodmer.[17] For the coupling of pions to nucleus we use the pseudo-vector coupling to avoid the unphysical S-wave interaction of the pseudo-scalar (γ_5) coupling. Our effective Lagrangian density is then

$$\begin{aligned}\mathcal{L}_{eff} = {} & \bar{\psi}\left(i\not{\partial} - g_V\not{V} - (m_N - g_s\sigma) - g_\pi\gamma_5\gamma^\mu\underset{\sim}{\tau}\cdot\partial_\mu\underset{\sim}{\pi}\right)\psi \\ & + \frac{1}{2}\left(\partial_\mu\sigma\partial^\mu\sigma - m_s^2\,\sigma^2\right) + \frac{1}{2}\left(\partial_\mu\underset{\sim}{\pi}\partial^\mu\underset{\sim}{\pi} - m_\pi^2\,\pi^2\right) \\ & - \frac{1}{4}F_{\mu\nu}F^{\mu\nu} + \frac{1}{2}m_V^2\;V_\mu V^\mu - U(\sigma) \qquad . \end{aligned} \tag{17}$$

where the scalar potential density is

$$U(\sigma) = \left(\frac{1}{3}\,b\,m_N + \frac{1}{4}\,c\,g_s\sigma\right)(g_s\sigma)^3 \qquad . \tag{18}$$

Here m_N is the nucleon mass. The mean field equations are then[2]

$$m_s^2\bar{\sigma} = g_s\langle\bar{\psi}\psi\rangle - \langle\frac{dU}{d\sigma}\rangle \quad , \tag{19a}$$

$$m_V^2\bar{V}_\mu = g_V\langle\bar{\psi}\gamma_\mu\psi\rangle \quad , \tag{19b}$$

$$(\Box + m_\pi^2)\langle\underset{\sim}{\pi}(x)\rangle = g_\pi\partial^\mu\langle\bar{\psi}(x)\,\gamma_5\gamma_\mu\underset{\sim}{\tau}\,\psi(x)\rangle \quad , \tag{19c}$$

$$\left\{i\not\partial - g_V\not{\bar{V}} - (m_N - g_s\bar{\sigma}) - g_\pi\gamma_5\gamma^\mu\underset{\sim}{\tau}\cdot\partial_\mu\langle\underset{\sim}{\pi}(x)\rangle\right\}\psi(x) = 0 \quad . \tag{19d}$$

where $\bar{\sigma} = \langle\sigma\rangle$ and $\bar{V}_\mu = \langle V_\mu\rangle$ are independent of x for homogeneous nuclear matter.

The field configuration corresponding to the normal phase of symmetric nuclear matter is $\{\bar{\sigma}\neq 0,\ \bar{V}_\mu = \delta_{\mu 0}\bar{V}_0,\ \langle\underset{\sim}{\pi}\rangle = 0,\ \bar{\rho}_\mu = 0\}$. This is the field configuration considered by Walecka et al.[14,15] Since Eqs. (19a-d) form a nonlinear system of equations for the mean field, we can seek other (abnormal) field configurations which also solve Eq. (19). In particular, we investigate under what conditions a pion condensed solution exists of the form

$$\langle\underset{\sim}{\pi}(x)\rangle = \bar{\pi}(\underset{\sim}{u}\cos kx + \underset{\sim}{v}\times\underset{\sim}{u}\sin kx) \quad , \tag{20}$$

where $\underset{\sim}{u}$ and $\underset{\sim}{v}$ are two orthonormal isospin vectors. The case $\underset{\sim}{u} = (1,0,0)$, $\underset{\sim}{v} = (0,0,1)$ corresponds to the charged running wave case: $\sqrt{2}\,\langle\pi_\pm\rangle = \bar{\pi}\,e^{\pm ikx}$, $\langle\pi_0\rangle = 0$. In symmetric nuclear matter, the actual orientation of $\underset{\sim}{u}$ and $\underset{\sim}{v}$ in isospin space plays no role in the self consistency equations, since there is no preferred direction in isospin space. Thus, if Eq. (20) is a self-consistent field for some particular $\underset{\sim}{u}$ and $\underset{\sim}{v}$, then it is a self solution with the same $\bar{\pi}$ but with arbitrary

$\underset{\sim}{u}$ and $\underset{\sim}{v}$ subject to $\underset{\sim}{u} \cdot \underset{\sim}{v} = 0$.

The key trick to solving the space-time-dependent Dirac equation in Eq. (19d) for a π condensed field, Eq. (20), is that this space-time dependence of $\langle \underset{\sim}{\pi}(x) \rangle$ can be transformed away with a local isospin gauge transformation:

$$\underset{\sim}{\tau} \cdot \partial_\mu \langle \underset{\sim}{\pi}(x) \rangle = \bar{\pi} k_\mu \, R_v(kx) \, \underset{\sim}{\tau} \cdot \underset{\sim}{v} \times \underset{\sim}{u} \, R_v^+(kx) \quad , \tag{21}$$

where

$$R_v(kx) = e^{-\frac{i}{2}(kx)\, \underset{\sim}{\tau} \cdot \underset{\sim}{v}} \quad . \tag{22}$$

Defining the transformed Dirac field ψ_v by

$$\psi(x) = R_v(kx) \, \psi_v(x) \quad , \tag{23}$$

Eq. (19d) reduces to a space-time *independent* Dirac equation for ψ_v,

$$\left\{ i\not{\partial} - g_v \not{\bar{v}} - (m_N - g_s \bar{\sigma}) + \not{k} \underset{\sim}{\tau} \cdot \left(\frac{1}{2} \underset{\sim}{v} + g_\pi \bar{\pi} \gamma_5 (\underset{\sim}{v} \times \underset{\sim}{u}) \right) \right\} \psi_v(x) = 0 \quad . \tag{24}$$

Therefore, the transformed quasiparticle wavefunctions are simple plane waves times complicated spinors $\bar{u}_v^i$. Fortunately, we never need to compute these spinors, since we only need to compute expectation values of currents, $\langle \bar{\psi} \Gamma \psi \rangle$. These expectation values can be computed using standard propagator techniques as follows:

$$\begin{aligned} \langle \bar{\psi}(x) \Gamma \psi(x) \rangle &= \sum_{\omega_i < E_F} \bar{u}_v^i \, R_v^+(kx) \Gamma \, R_v(kx) \, u_v^i \\ &= \sum_{\omega_i < E_F} \mathrm{Tr} \left\{ R_v^+(kx) \Gamma \, R_v(kx) \, (u_v^i \bar{u}_v^i) \right\} \\ &= \sum_{\omega_i < E_F} \mathrm{Tr} \left\{ R_v^+(kx) \Gamma \, R_v(kx) \, \underset{p_0 = \omega_i}{\mathrm{Res}} \, S_v(p_0, \underset{\sim}{p}_i) \right\} \end{aligned} \tag{25}$$

where $S_v(p_o,\underset{\sim}{p})$ is the transformed quasiparticle propagator. With some algebra, we can compute the transformed propagator as

$$S_v(p_o,\underset{\sim}{p}) = \left\{\not{p}' - m^* + \not{k}\underset{\sim}{\tau}\cdot\left(\frac{\underset{\sim}{v}}{2} + g_\pi\bar{\pi}\gamma_5\underset{\sim}{v}\times\underset{\sim}{u}\right)\right\}^{-1}$$

$$= \frac{1}{D(p)}\left\{p_0'^2 - \varepsilon^2 - (p'k)\underset{\sim}{\tau}\cdot\underset{\sim}{v} - 2g_\pi\bar{\pi}[(p'k) + m^*\not{k}]\gamma_5\underset{\sim}{\tau}\cdot\underset{\sim}{v}\times\underset{\sim}{u}\right\}$$

$$\times\left\{\not{p}' + m^* + \not{k}\underset{\sim}{\tau}\cdot\left[\frac{1}{2}\underset{\sim}{v} - g_\pi\bar{\pi}\gamma_5\underset{\sim}{v}\times\underset{\sim}{u}\right]\right\} \quad , \tag{26}$$

where

$$p_\mu' = p_\mu - g_v\bar{V}_\mu \quad ,$$

$$m^* = m_N - g_s\bar{\sigma} \quad ,$$

$$\varepsilon^2 = |\underset{\sim}{p}'|^2 + m^{*2} - \left(\frac{1}{4} + g_\pi^2\bar{\pi}^2\right)(kk) \quad , \tag{27}$$

and

$$D(p_o,p) = (p_o'^2 - \varepsilon^2)^2 - (p'k)^2 - 4g_\pi^2\bar{\pi}^2((p'k)^2 - m^{*2}(kk)) . \tag{28}$$

The quasiparticle spectrum $\omega(\underset{\sim}{p})$ follows from the singularities of $S(p_o,\underset{\sim}{p})$, i.e., from

$$D(\omega(\underset{\sim}{p}),\underset{\sim}{p}) = 0 \quad . \tag{29}$$

For $\bar{\pi}\to 0$, $\omega(\underset{\sim}{p}) = g_v\bar{V}_o + ((\underset{\sim}{p}\pm\underset{\sim}{k}/2)^2 + m^{*2})^{\frac{1}{2}}$, and the Fermi surface is composed of two Fermi spheres which are displaced by $\pm\underset{\sim}{k}/2$ from the origin. This displacement is, however, only an artifact of the gauge transformation Eq. (22) and (23), and leads to no physical baryon or isospin currents. When $\bar{\pi}\neq 0$ is a self-consistent solution of the mean field equations, Eq. (19), there appears a gap in the quasiparticle spectrum at $\underset{\sim}{p} = 0$ and

the Fermi surface acquires a more complex peanut shape.

Having found $S_v(p_o,\underset{\sim}{p})$ and the quasiparticle spectrum, $\omega(\underset{\sim}{p})$, we can now use Eq. (25) to calculate all the necessary source currents appearing on the right-hand side of Eqs. (19a-c). These source currents are functions of the unknown fields $\{\bar{\sigma}_v, \bar{V}_o, \bar{\pi}\}$, and thus Eq. (19a-c) poses a self-consistency problem. Fortunately, for a fixed Fermi energy E_F, only the $\bar{\sigma}$ and $\bar{\pi}$ equations are coupled to each other. The numerical procedure is thus to fix E_F, find $\bar{\sigma}(E_F)$ and $\bar{\pi}(E_F)$ from Eq. (19a,c), then use those values in computing $\bar{V}_o(E_F)$ from Eq. (19b), and finally to calculate the baryon density $\rho_B(E_F)$ and the energy density $\mathcal{E}(E_F)$.

The final binding energy per baryon $E/A = \mathcal{E}(E_F)/\rho_B(E_F)$ depends on the five parameters

$$g_s/m_s\ , \qquad g_v/m_v\ , \qquad b\ , \qquad c\ , \qquad g_\pi\ .$$

The first four parameters are chosen to reproduce the known bulk properties of nuclear matter: (1) $E/A = -15.96$ MeV at $\rho_o = 0.145\ \mathrm{fm}^{-3}$, (2) $\partial(E/A)/\partial\rho = 0$ at ρ_o, and (3) the incompressibility $K = 9\rho_o^2\partial^2(E/A)/\partial\rho^2 = 200\text{-}300$ MeV at ρ_o. The fourth constraint that we introduce to fix the first four coupling constants is to require that $B/A = 0$ at some density between $2\rho_o - 3\rho_o$. This last constraint is a statement of our guess about the softness of the equation of state at higher densities. For g_π we take an effective value motivated by our analysis of the pion self energy via Eqs. (13) and (14).

In order to clarify the relationship between MFA and the RPA method discussed previously, we show in Appendix A that the relativistic mean field equations reduce to the relativistic RPA equations as the field

strength vanishes. In particular, in the $\langle\underset{\sim}{\pi}(x)\rangle \to 0$ limit, Eq. (19c) reduces to

$$(-k^2 + m_\pi^2 + \Pi_{rel}(k))\bar{\pi} = 0 \quad , \tag{30}$$

where Π_{rel} is the relativistic Lindhard function [Eq. (A.13) of Appendix A],

$$\Pi_{rel}(k) = -2ig_\pi^2 \int \frac{d^4p}{(2\pi)^4} \mathrm{Tr}\left(\not{k}\gamma_5 S(p) \not{k}\gamma_5 S(p+k)\right) \quad , \tag{31}$$

with $S(p) = (\not{p} - g_v\not{v} - m^* + i\varepsilon\,\theta(E_F - p_o))^{-1}$. When $p_F \ll m^*$, Π_{rel} reduces to the non-relativistic Lindhard function as in Eq. (9) (with $F_{\pi N} = 1$). However, recoil and relativistic kinematics in Eq. (31) lead to correction of order $(p_F/m^*)^2, (k/m^*)^2 \sim 10\text{-}20\%$ to that non-relativistic self energy. Therefore, the g_π used in Eq. (19c) may differ by ~10% from f_{eff} in Table 1. A detailed study comparing Eq. (31) to the non-relativistic Lindhard function is currently in progress.

In Figs. 2 and 3, we illustrate the equation of state for two sets of parameters (g_s, g_v, b, c) that yield reasonable equations of state in the normal phase, $\langle\pi\rangle = 0$. For sufficiently large g_π, self-consistent pion condensate solutions, Eq. (20), are also found that lower the ground state energy. As we lower g_π from the free space value, $f_\pi = 1.41$ fm, to simulate correlations, Δ production, and form factors as in Eq. (14), we find that the critical density increases and the condensate energy lowers.

The difference between the equations of state in Figs. 2 and 3 is due mainly to the difference between effective mass, $m^*(\rho)$, for each case. Recall from Section II that the driving force $\Pi \propto m^*(\rho)$. In Fig. 4 we show $m^*(\rho)$ corresponding to each case.

In our Lagrangian, Eq. (17), the $m^*(\rho)$ is controlled indirectly by the nonlinear σ interactions in Eq. (18). For $b = c = 0$, corresponding to the Walecka model, $m^*(\rho)$ is strongly density dependent and has a rather small value, ~0.6 m_N. Associated with this small m^* is a rather high incompressibility, $K \sim 500$ MeV, which follows from the large values g_s/m_s and g_v/m_v needed to reproduce the binding and saturation density. By introducing the nonlinear interactions of Eq. (18), which are equivalent to three and four body forces, we can lower g_s/m_s and g_v/m_v. Since g_v/m_v controls the magnitude of m^* while g_s/m_s controls the density dependence of m^*, by lowering g_s/m_s and g_v/m_v we increase the magnitude of m^* and reduce its density dependence. This is what we find in Fig. 4. The larger the values of b and c, the smaller are the values of g_s/m_s and g_v/m_v needed to reproduce the stauration properties, and consequently $m^*(\rho)$ is larger and less density dependent. Also, by lowering g_s/m_s and g_v/m_v, we see from Figs. 2 and 3 that the equation of state becomes softer. Therefore, there is a correlation between larger three and four body forces, larger and less density dependent $m^*(\rho)$, a softer equation of state, a lower critical density, and greater condensation energy.

Another important difference between the parameter sets in Figs. 2 and 3 is the minimum value of g_π for which no condensate solution exists. For Fig. 2 with the smaller b,c, no condensate solutions were found for $g_\pi < 1.18$ fm. For the larger b,c in Fig. 3, the critical density simply gets shifted toward higher densities as g_π is lowered. Comparing to Table 1 for the expected renormalization of g_π due to correlations, Δ production and form factors, we can say that in the first case π condensation is very unlikely to occur at all, while in the second case a condensate

can develop at higher densities $\gtrsim(2\text{-}3)\rho_0$.

We conclude that pion condensation in symmetric nuclear matter can be made consistent with the bulk properties of nuclear if the effective mass is large ($m^* \gtrsim 0.9$), which in our model occurs when sufficiently large three and four body forces exist. To gauge how large these forces are in the case of Fig. 3, we can compute from Eq. (18) the net contribution of these many body forces to the energy per nucleon at normal density. For these parameters of Fig. 3 this is

$$\left(\frac{E}{A}\right)_{3,4\ \text{body}} = \frac{U(\sigma)}{\rho_0} = -46\ \text{MeV} \quad , \tag{32}$$

which is quite large. However, slight variations of b,c yielding nearly identical results to Fig. 3 can result in a factor of 10 smaller value of Eq. (32).

Next, we contrast our results to calculations using the chiral model[13] where m^* is fixed to be m_N. In Fig. 5 we compare the condensation energy, Eq. (16), calculated in Ref. 13 to those obtained from Figs. 2 and 3 for g_π chosen to give approximately the same critical density. As expected, the chiral model with the much larger driving force tends to give a much higher condensation energy that increases rapidly with density. We conclude that self-consistency and compatibility with the bulk nuclear properties are very strong constraints on the existence and persistence of the condensate phase.

Finally, we wanted to know the expected magnitude of the pion field for various g_π. Typically, $\bar{\pi}$ in Eq. (20) turns out to be on the order of $0.1\ m_\pi$. In order to get a feeling for this number, we should compare the amplitude of spin-isospin oscillations to the normal baryon density. From Eq. (19c), we can convert $\bar{\pi}$ into a magnitude of $\langle\bar{\psi}\gamma_5\gamma_3(\underset{\sim}{\tau}\cdot\underset{\sim}{u})\psi\rangle$ for $\underset{\sim}{k} = 2m_\pi\,\hat{e}_3$ as

$$<\bar{\psi}\gamma_5\gamma_3(\underset{\sim}{\tau}\cdot\underset{\sim}{u})\psi> = \frac{(k^2+m_\pi^2)}{g_\pi k}\,\bar{\pi} \quad , \tag{33}$$

For $\bar{\pi} = 0.1\ m_\pi$, $g_\pi = 1/m_\pi$, the right-hand side is $0.25\ m_\pi^3$ which is about one-half the normal baryon density, $\rho_0 \approx 0.5\ m_\pi^3$. Thus, sizeable oscillations of the spin-isospin density are possible. It is important to note, however, that unlike the neutral condensate, the class of condensate solutions considered in Eq. (20) do not lead to density oscillations. The baryon density is uniform; only the spin-isospin density oscillates. In Fig. 6 we plot the ratio of the spin-isospin density $<\bar{\psi}\gamma_5\gamma_3\tau_3\psi>$ to the baryon density $<\bar{\psi}\gamma_0\psi>$ for a case with $g_\pi = 1$ fm in Fig. 3. Note that non-relativistically $<\bar{\psi}\gamma_5\gamma_3\tau_3\psi> \approx \rho(p\uparrow) + \rho(n\downarrow) - \rho(p\downarrow) - \rho(n\uparrow)$ is the spin-isospin density, where $\rho(p\uparrow)$ is the density of protons with spin pointed along the z axis, etc. On the other hand, $\rho = <\bar{\psi}\gamma_0\psi> \approx \rho(p\uparrow) + \rho(n\downarrow) + \rho(p\downarrow) + \rho(n\uparrow)$ is independent of x. The ratio $R_{53} = <\bar{\psi}\gamma_5\gamma_3\tau_3\psi>/<\bar{\psi}\gamma_0\psi>$ in Fig. 6a measures the magnitude of the spin-isospin density oscillations in the condensed state. We see that for $\rho \gtrsim 2\rho_0$ that $R_{53} \approx 0.5$. The corresponding oscillations of the densities $\rho(p\uparrow)+\rho(n\downarrow)$ and $\rho(p\downarrow)+\rho(n\uparrow)$ are illustrated in Fig. 6b.

It is remarkable to note in Fig. 6a that although the condensate energy is very small, $\lesssim 3$ MeV, the spin-isospin oscillations are about as large as they can possibly get. In fact, R_{53} only increases to 0.85 when $g_\pi = 1.41$, even though condensate energy is about 10 times larger. This has important consequences when considering dynamical effects of pionic instabilities. Clearly, the very slight softening of the equation of state, $E/A(\rho)$, due to condensation would have very little effect in

hydrodynamic calculations. However, the large spin-isospin fluctuations can lead to critical scattering phenomena as discussed below, which we could hope to observe. In the next section we study the dynamical consequences associated with pionic instabilities.

III. DYNAMICAL EFFECTS IN NUCLEAR COLLISIONS

A. Pionic Instabilities vs. Pion Condensation

Having reviewed the underlying theory of pion condensation, we now turn to what experimental signatures such pion field coherence phenomena could lead to in relativistic nuclear collisions. For possible consequences in neutron star cooling rates, see Baym.[1]

In discussing dynamical effects it is important to make a distinction between pion condensation, which is an equilibrium phenomena, and what I call pionic instabilities,[7] associated with non-equilibrium states of nuclear matter. The former is analogous to the anti-ferromagnetic phase of certain materials, while the latter is analogous to plasma instabilities in colliding plasmas. As emphasized in Ref. 7, pionic instabilities may occur even if pion condensation does not. For example, a finite tempera-

ture plasma may be stable with respect to spontaneous growth of charge density waves, yet a two stream plasma may be unstable in these types of excitations. The difference in the two cases lies entirely in the form of the dielectric function (or equivalently, the photon self energy in the plasma). The same difference can occur for pion fields in nuclear matter.

To compare $\Pi(k)$ for equilibrium and non-equilibrium systems, consider the nucleon-hole polarization energy, $\Pi_N(k)$, given by Eq. (11), with $\omega_h - \omega_p = -(\underset{\sim}{p}\cdot\underset{\sim}{k} + k^2/2)/m^*$. For $T=0$ the sum over $\underset{\sim}{q}$ is restricted to the occupied states distributed as $n_o(\underset{\sim}{p}) = \theta(p_F - p)$. Let $\Pi_N^o(k)$ denote the self energy in this case, Eq. (9). Now consider two interpenetrating nuclear beams as in nuclear collisions, where the initial distribution of occupied states is given by

$$n(\underset{\sim}{p}) = n_o(\underset{\sim}{p} - \underset{\sim}{p}_{cm}) + n_o(\underset{\sim}{p} + \underset{\sim}{p}_{cm}) \quad . \tag{34}$$

Equation (34) describes two displaced Fermi spheres. The net baryon density of the system is $\rho = 2\rho_o$. For high enough center-of-mass momentum p_{cm}, Pauli blocking can be ignored between the two Fermi spheres. Then by simply changing variables, $\underset{\sim}{q}' = \underset{\sim}{q} \pm \underset{\sim}{p}_{cm}$, in Eq. (11) with $n(p)$ given by Eq. (34) we obtain

$$\Pi_N(\omega,k) = \Pi_N^o\left(\omega + \frac{\underset{\sim}{p}_{cm}\cdot\underset{\sim}{k}}{m^*}, \underset{\sim}{k}\right) + \Pi_N^o\left(\omega - \frac{\underset{\sim}{p}_{cm}\cdot\underset{\sim}{k}}{m^*}, \underset{\sim}{k}\right) \quad . \tag{35}$$

For $\omega = 0$ and $\underset{\sim}{k} \perp \underset{\sim}{p}_{cm}$, we see therefore that

$$\Pi_N(0,\underset{\sim}{k}) = 2\Pi_N^o(0,\underset{\sim}{k}) \quad . \tag{36}$$

This should be contrasted to the case of equilibrium nuclear matter at

the same density, $2\rho_0$, for which Π_N is only $2^{1/3}$ larger than Π_N^0 as seen from Eq. (9). Therefore, the non-equilibrium aspect of the streaming nuclear matter described via Eq. (31) has lead to a 60% enhancement of the driving force via Eq. (33) for $\underset{\sim}{k} \perp \underset{\sim}{p}_{cm}$ relative to the equilibrium case. As shown in Ref. 7, for $\underset{\sim}{k}$ not perpendicular to $\underset{\sim}{p}_{cm}$, this enhancement is reduced. Translated into an effective πNN coupling, g_π, non-equilibrium effects thus lead to ~30% enhancement. As seen in Figs. 2 and 3, such an enhancement of g_π can make it much more favorable for pionic instabilities to occur. Thus in this sense it may be advantageous to study non-equilibrium nuclear systems, such as those arising in nuclear collisions, to look for signatures of pion field coherence.

As to what signatures we should look for, we first review the basic dynamical consequences of pionic instabilities.[7] Collective instabilities effect the dynamics in two essential ways: (1) through the growth of collective fields, $\langle \underset{\sim}{\pi}(\underset{\sim}{x},t)\rangle$, and (2) through the modification of two-body scattering rates. These two aspects of collective instabilities are intimately interrelated through the nature of the pion spectrum in the medium. There are, in general, several branches of the pion spectrum in nuclear systems.[1,7] First there is a particle-hole branch with pion energies in the range $0 < \omega \lesssim p_F k/m$. These correspond to collective excitations with pion quantum numbers that decay primarily to particle-hole pairs. At high densities there may also be a condensate branch with $\omega = 0$ which represents unstable collective modes involving coherent many particle-many hole excitations. There is also a quasifree branch corresponding to almost on-shell pions with $\omega \approx m_\pi$ and a Δ_{33}-N hole branch with $\omega \approx 2.4\, m_\pi$. All these difference branches, $\omega_i(\underset{\sim}{k})$, just

correspond to different singularities of the pion propagator, $\Delta^{-1}(\omega_i(\underset{\sim}{k}),\underset{\sim}{k}) = 0$, for fixed k.

If we consider the decay of the system in terms of "$\pi^+\pi^-$" pair production, then because there are many branches of the π spectrum in nuclear matter, several dynamical processes can be described at once on the same footing. The formalism for such a calculation was derived in Ref. 7. The basic result is that the total decay rate per unit volume, Γ/V, of a system can be computed from the imaginary part of the correlation energy with the result that

$$\frac{\Gamma}{V} = \mathrm{Re}\int \frac{3d^4k}{(2\pi)^4} \log\ \varepsilon(\omega,\underset{\sim}{k}) \quad , \tag{37}$$

where the "dimesic" function is given by

$$\varepsilon(\omega,\underset{\sim}{k}) = 1 - \left[\frac{1}{\omega^2 - \underset{\sim}{k}^2 - m_\pi^2} + \frac{g'}{|\underset{\sim}{k}|^2}\right]\left[\Pi_N(\omega,\underset{\sim}{k}) + \Pi_\Delta(\omega,\underset{\sim}{k})\right] . \tag{38}$$

It is easy to see that $\varepsilon(\omega,\underset{\sim}{k}) = 0$ whenever $\Delta^{-1}(\omega,\underset{\sim}{k}) = 0$, and hence all branches of the pion spectrum are incorporated in ε. Detailed study[7,19] of Eq. (37) shows that Γ can be decomposed into a sum of partial widths into different channels as

$$\Gamma = \Gamma_0 + \Gamma_{el} + \Gamma_{inel} + \Gamma_{\pi'} \tag{39}$$

where Γ_0 is the rate of condensate pion pair creation, Γ_{el} and Γ_{inel} are the two-body elastic and inelastic scattering rates, and $\Gamma_{\pi'}$ is the rate of quasifree pion production.

A model calculation of the magnitude of Γ_i was reported in Ref. 19. We reproduce here for illustration typical results corresponding to nuclear collisions with beam energy $E_L = 380$ and 1040 MeV/nucleon.

TABLE 2. Partial decay rates per unit volume (from Ref. 19).

E_L (MeV/A)	Γ/V (m_π^4)	Γ_o/V (m_π^4)	Γ_{el}/V (m_π^4)	Γ_{inel}/V (m_π^4)	$\Gamma_{\pi'}/V$ (m_π^4)
380	0.72	0.11	0.37	0.24	0.10
1040	1.14	0.12	0.27	0.72	0.13

For comparison note that if the decay of n(p) in Eq.(34) were purely due to two-body scatterings with cross section $\sigma_{NN} \approx 40$ mb, then $\Gamma/V = \rho^2 \sigma_{NN} v_{rel} = 0.063(0.079)\ fm^{-4} = 0.25(0.31)\ m_\pi^4$ for $E_L = 380(1040)$ MeV/A, respectively. Thus, there is a factor ~3 enhancement of the decay rate due to pionic instabilities. This enhancement is due to the combined effects of the growth of collective fields via $\Gamma_o + \Gamma_{\pi'}$ and the enhancement of the scattering rate $\Gamma_{el} + \Gamma_{inel}$ due to critical scattering phenomena.

The question is how could we search for evidence of these enhancements via nuclear collisions? The main problem is that higher Γ means faster equilibration time. Once the momenta distributions are thermalized then the memory of the possibly interesting dynamical path is lost. As we shall see, it is not easy to uncover clean signatures of pionic instabilities. The two experiments described below are our best hope at the present to look for such phenomena. First, we describe the Tanihata, et al's large-angle proton correlation experiment to search

for critical scattering phenomena. Second, we describe Crowe et al's small-angle pion correlation experiment to search for evidence of the coherent pion fields produced via $\Gamma_{\pi'}$.

B. Critical Scattering Phenomena

The enhancement of $\Gamma_{el} + \Gamma_{inel}$ in Table 2 is due to the interaction of the exchanged pions with the medium. Thus, instead of the free pion propagator $\Delta_0(\omega,\underset{\sim}{k})$, the medium-modified propagator $\Delta(\omega,k)$ enters into the amplitude for scattering, as illustrated below for the effective differential cross section

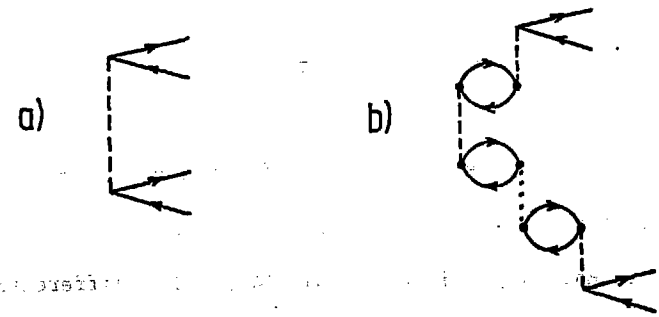

The scattering rates in the medium get enhanced because the pion can propagate further for certain critical momenta k, hopping from one nucleon to the next — the "skipping stone" effect. This larger propagation amplitude leads to an enhanced effective two-body cross section, $d\sigma_{eff}$, that differs from the free space cross section, $d\sigma_0$, by a multiplicative polarization factor,[7,19] $P(\omega,\underset{\sim}{k})$, as

$$\frac{d^3\sigma}{d^3k}\ \text{eff}\ \left(N(\underset{\sim}{p}_1) + N(\underset{\sim}{p}_2) \to A(\underset{\sim}{p}_1 + \underset{\sim}{k}) + B(\underset{\sim}{p}_1 - \underset{\sim}{k})\right) = P(\Delta\omega,\underset{\sim}{k})\ \frac{d^3\sigma_0}{d^3k}\ (NN \to AB) \tag{40}$$

where $\Delta\omega$ is the energy transfer and $\underset{\sim}{k}$ is the momentum transfer in the

scattering of the two nucleons, N, of momenta $\underset{\sim}{p}_1$ and $\underset{\sim}{p}_2$ to states A and B. Here A,B can be either nucleons or Δ_{33} resonances.

The expression for $P(\omega,\underset{\sim}{k})$ involves the dimesic function, Eq. (38), and the differential scattering rate $\gamma_0(\omega,\underset{\sim}{k})$, that measures the number of binary collisions with energy-momentum transfer $(\omega,\underset{\sim}{k})$ in the *absence* of the polarization effect:

$$P(\omega,\underset{\sim}{k}) = -\frac{1}{\gamma_0(\omega,k)}\log\left\{1-\frac{\gamma_0(\omega,k)}{|\varepsilon(\omega,k)|^2}\right\} . \tag{41}$$

It can be proven[7] that $0 < \gamma_0/|\varepsilon|^2 < 1$. Furthermore, for $\gamma_0 \to 0$,

$$P(\omega,\underset{\sim}{k}) \xrightarrow[\gamma_0\to 0]{} \frac{1}{|\varepsilon(\omega,k)|^2} , \tag{42}$$

which is the Balescu-Lenard result for the effective cross section in plasmas. Thus, if the collision rate using free space cross sections is low $(\gamma_0(\omega,\underset{\sim}{k}) \to 0)$, then Eq. (41) reduces to Eq. (42). The differential scattering rate, $\gamma_0(\omega,k)$, has the following physically intuitive form in terms of the free space $d^3\sigma_0/dk^3(NN\to AB)$ differential cross section:

$$\gamma_0(\omega,\underset{\sim}{k}) = \frac{(2\pi)^4}{3}\sum_{A,B=N,\Delta}\int \frac{4d^3p_1}{(2\pi)^3}\,\frac{4d^3p_2}{(2\pi)^3}\left\{n(p_1)\,n(p_2)\right.$$

$$\times\ \delta\big(\omega+\varepsilon_N(p_1)-\varepsilon_A(p_1+k)\big)\times\delta\big(\omega+\varepsilon_N(p_2)-\varepsilon_B(p_2-k)\big)$$

$$\left.\times\ \frac{d^3\sigma_0}{dk^3}\big(N(p_1)+N(p_2)\to A(p_1+k)+B(p_2-k)\big)\right\} . \tag{43}$$

(Pauli blocking terms have been suppressed here.) The total scattering

rate per unit volume with free space cross sections is then

$$\Gamma^{o}_{scat}/V = \rho^2 \langle \sigma_o v_{rel} \rangle = \frac{3}{2} \int \frac{d^4k}{(2\pi)^4} \gamma_o(\omega,\underset{\sim}{k}) \quad . \quad (44)$$

The sum over A,B in Eq. (43) is over final nucleon and Δ states. In the RPA ring approximation used in deriving Eq. (41), $d^3\sigma_o/dk^3$ in Eq. (43) is proportional to the free pion propagator, $|\Delta_o(\omega,\underset{\sim}{k})|^2$. If there exists a condensate mode $\underset{\sim}{k}_c$ such that $|\varepsilon(0,\underset{\sim}{k}_c)|^2 = 0$, then $P(0,\underset{\sim}{k}_c) \to \log \infty$. Furthermore, if the momentum transfer $\underset{\sim}{k}_c$ is kinematically allowed, then the effective differential cross section will diverge at that critical momentum transfer. This is called critical scattering phenomena.

For completeness we show in Fig. 7, a calculated example[7] for $P(0,k) = d\sigma_{eff}/d\sigma_o$. The main feature is the large enhancement for $k_c \sim 2m_\pi \pm m_\pi$. The actual magnitude of the enhancement depends sensitively on the momenta $\underset{\sim}{p}_1$ and $\underset{\sim}{p}_2$ of the nucleons,[7] but the enhancement is always largest for $k \sim 2m_\pi$ and $\omega = 0$.

The first place we would look for such critical scattering phenomena is the single proton inclusive cross section in the kinematic region of quasi-elastic scattering. However, several factors tend to camouflage or obscure any peak structure resulting from critical scattering:

(1) The background due to multiple collision components of the inclusive yield;

(2) The background due to direct, knock-out collisions from the nuclear surface;

(3) The background due to projectile and target fragmentation;

(4) The coincidence of $k_c \approx p_F$ and $\Delta k_c \approx p_F$ and the additional broadening of Δk_c due to Fermi motion.

To understand the first two sources of background, we write, as in Ref. 20, the inclusive cross section $E\, d^3\sigma/dp^3$ as a multiple cluster series

$$E\,\frac{d^3\sigma}{dp^3} = \sum_{M,N=1}^{A_P,A_T} \sigma(M,N)\, F_{MN}(\underset{\sim}{p}) \quad , \tag{45}$$

where $\sigma(M,N)$ is the weight associated with multiple collision of M projectile P nucleons with N target T nucleons, and $F_{MN}(\underset{\sim}{p})$ is the momentum distribution (normalized to M+N) associated with this multi-nucleon cluster scattering. For $M+N > 4$, F_{MN} rapidly approaches[20] the thermal limit relatively independent of the forms of the two-body cross section. Thus, only the $(M,N) = (1,1)$ and possibly the (1,2) and (2,1) contributions to Eq. (45) are likely to carry the signature of critical scattering phenomena. However, recent calculations of Knoll[20] indicate that the percentage of (1,1) contribution to total *integrated* yield for Ar+Ar is only 6% for impact parameter averaged cross sections and 4% for central triggered reactions. Of course, the relative importance of the (1,1) contribution for a particular point in phase space $(p_{\parallel}, p_{\perp})$ depends on how close $(p_{\parallel}, p_{\perp})$ is to the quasi-elastic kinematic region. Nevertheless, the single collision component tends to remain a small fraction of the single inclusive yield. For the lightest systems, C+C, the knock-out fraction may reach 50% in the quasi-elastic region due to the large diffuse surface. However, then the second source of background becomes important. Most of the knock-out contribution occurs then from the surface regions of the nuclei. In Ref. 21, it was estimated that most of the knock-out yield comes in fact from regions of the nuclear surface with density $\rho < 0.2\,\rho_0$. This means that the bulk of the knock-

out cross section occurs outside the high density region, so that polarization effects are likely to be small, $P(\omega,k) \approx 1$. Calculations are currently in progress to find out what fraction of knock-out comes from the high density region. We expect this fraction to be quite small. Therefore, we see that the background due to multiple collisions and nuclear surface knock-out nucleons will diminish greatly the chance to observe the critical scattering peak in $E\, d^3\sigma/dp^3$. In fact, points (3) and (4) lead to further suppresion of the peak.

To increase the (1,1) component and remove at least par: of the multiple scattering background, we turn now to the pp correlation experiment of Nagamiya et al[22] and Tanihata et al.[23] The basic idea here is to require a coincidence between two protons in the kinematic region of the knock-out. In Fig. 8, the quasi-elastic kinematic region is indicated by the dashed circle going through the projectile and target momenta in the CM frame. A knock-out scattering will result in placing two nucleons on this circle such that the line joining them goes through the CM point. Indicated by the dashed region is the acceptance of a tag counter R that records one proton with cm angle $\theta_{cm} \approx 90°$ and azimuthal angle $\phi = 180°$. The spectrometer is then set up to record all protons with azimuthal angle $\phi = 0$ that occur in coincidence with the tag counter. In addition, there is tag counter U set up to record protons with ($\theta_{cm} \approx 90°$, $\phi = 90°$), out of the plane defined by tag R and the spectrometer. Coincidence between the spectrometer and tag U can only occur because of the background due to multiple scattering. An in-to-out of plane correlation function is then defined as

$$C(\theta_{cm},p_{cm}) = \frac{Y_R(\theta_{cm},p_{cm},\theta_R=90°,\ \phi_R=180°)}{Y_U(\theta_{cm},p_{cm},\theta_U=90°,\ \phi_U=90°)} \quad , \qquad (46)$$

where $Y_I\ (\theta_{cm}, p_{cm}, \theta_I, \phi_I)$ is the coincidence rate between a proton measured with tag I set at CM angles (θ_I,ϕ_I) and the spectrometer proton measured at cm angle θ_{cm}, $\phi = 0$ and momentum p_{cm}. The contours in Fig. 8 display this measured correlation function. We can see clearly the quasi-elastic peak at $\theta_{cm} = 90°$, $\phi = 0$. As expected, going from C to Ar increases the multiple scattering background and, hence, decreases the quasi-elastic peak. Also note that the width of this peak is closely related to the Fermi momentum $p_F \approx 250$ MeV/c. To appreciate Fig. 8, recall[20,22] that the single inclusive cross section for $\theta_{cm} = 90°$ protons is smooth and structureless, with no evidence of the knock-out peak. The coincidence experiment, on the other hand, produced a clear signature of the knock-out contribution. The peak height of C in excess of 1 in Fig. 8 can be used to estimate the knock-out component[23] giving ≈50% in this configuration.

The next generation of correlation experiments proposed by Tanihata et al will study this knock-out component at different cm angles by moving the tag counters R and U to $\theta_R = \theta_U < 90°$(cm). The hope is that $\max(C-1) = f(\theta_R)$ will reveal the dependence of the effective differential elastic nucleon-nucleon cross section with cm angle θ_R. If this turns out to be the case (a theoretical problem currently under investigation by Knoll and Randrup), then this experiment can be used to look for signatures of critical scattering phenomena. The main problem will be to untangle the large background remaining from knock-out collisions in the low

density surface region, for which $P(\omega,k) \approx 1$. At present though, this experiment offers the best hope in the search for evidence of critical scattering phenomena in nuclear collisions.

C. Pion Field Coherence and Pion Interferometry[24]

We now discuss an alternate way to search for evidence of coherent pion phenomena via small angle identical pion correlation experiments. The study of such correlations is called pion interferometry, and is analogous to the well known Hanbury Brown-Tiss interferometry technique in quantum optics. There are two aspects of pion interferometry:

(1) The deduction of the space-time history of the pion source;

(2) The deduction of the degree of coherence of the pion field.

I will concentrate here on the second aspect.

The source of possible coherent pion fields in nuclear collisions is the time-dependent, collective spin-isospin current, $\underset{\sim}{J}_{5\mu}(x) = \langle\bar{\psi}\gamma_5\gamma_\mu\underset{\sim}{\tau}\psi\rangle$ that could arise if pionic instabilities occur. As we saw in Eq. (3c), the source of the pion field is actually

$$j(x) = g_\pi \partial^\mu \underset{\sim}{J}_{5\mu}(x) \quad . \tag{47}$$

In equilibrium, $j(\underset{\sim}{x},t) = j(\underset{\sim}{x})$ is independent of time (in symmetric nuclear matter) and no on-shell $(\omega = (k^2 + m_\pi^2)^{\frac{1}{2}})$ pions can be radiated. (In a condensate state, $\langle\pi(\underset{\sim}{x})\rangle \neq 0$, but there are no real pions in the system.) However, in non-equilibrium configurations as described, for example, by Eq. (34), pionic instabilities can lead to a time-dependent $j(\underset{\sim}{x},t)$, and hence on-shell pions can be produced. As we noted in Eq. (39),

both a condensate ($\omega = 0$) instability ($\Gamma_o \neq 0$) and a quasi-free pion ($\omega \approx m_\pi$) instability ($\Gamma_{\pi'} \neq 0$) can occur in non-equilibrium systems. Both instabilities grow at a charactersitic rate, γ, that is determined from the Γ_i. In particular, as shown in Ref. 7, we can write

$$\frac{\Gamma_o}{V} = \rho_{\pi c} \langle \gamma_c \rangle \quad , \qquad \frac{\Gamma_{\pi'}}{V} = \rho_{\pi'} \langle \gamma_{\pi'} \rangle \quad , \tag{48}$$

where $\rho_{\pi c}$ is the density of unstable condensate modes $\underset{\sim}{k}$ corresponding to a static $\omega = 0$ instability, and $\rho_{\pi'}$ is the density of unstable quasi-free pion modes with finite frequency $\omega \approx m_\pi$. Typical results of model calculations[7,19] indicate that $\rho_{\pi c} \approx \rho_{\pi'} \approx m_\pi^3$ and $\langle \gamma_c \rangle \approx \langle \gamma_{\pi'} \rangle \approx (0.1 - 0.2) m_\pi$.

Of course, in addition to this source of pions, the most important source is the usual $NN \to N\Delta$ mechanism included in Eq. (39) via Γ_{inel}. The pions produced by incoherent inelastic scatterings will, however, be described by a *chaotic field*.[24] The source current describing this incoherent, chaotic process can be written as

$$j_{ch}(x) = \sum_{i=1}^{N} e^{i\phi_i} j_\Delta(\underset{\sim}{x} - x_i) \quad , \tag{48}$$

where ϕ_i are random phases, x_i are N random inelastic scattering centers, distributed according to a density distribution $\rho(\underset{\sim}{x},t)$, and $j_\Delta(\underset{\sim}{x},t)$ describes the pion source current in one inelastic collision. If no pionic instabilities occur and the total current is given by Eq. (48), then as shown in Ref. 24, the single and double inclusive (negative) pion distributions are simply given by

$$p_1(\underset{\sim}{k}_1) = N|j_\Delta(\underset{\sim}{k},\omega_k)|^2$$

$$p_2(\underset{\sim}{k}_1,\underset{\sim}{k}_2) = N^2\ |j_\Delta(\underset{\sim}{k}_1,\omega_1)|^2\ |j_\Delta(\underset{\sim}{k}_2,\omega_2)|^2 \left\{1+|\rho(k_1-k_2)|^2\right\}, \quad (49)$$

where $\omega_k = (k^2 + m_\pi^2)^{\frac{1}{2}}$ and

$$j_\Delta(\underset{\sim}{k},\omega_k) = \int d^4x\ \frac{e^{i\omega_k t - i\underset{\sim}{k}\cdot\underset{\sim}{x}}}{(2\omega_k(2\pi)^3)^{\frac{1}{2}}}\ j_\Delta(\underset{\sim}{x},t) \quad . \quad (50)$$

Defining the two identical pion correlation functions as

$$R(\underset{\sim}{k}_1,\underset{\sim}{k}_2) = \frac{p_2(\underset{\sim}{k}_1,\underset{\sim}{k}_2)}{p_1(\underset{\sim}{k}_1)\ p_1(\underset{\sim}{k}_2)} \quad , \quad (51)$$

we see that $R = 1+|\rho(k_1-k_2)|^2$ measures the Fourier transform of the space-time distribution of inelastic scatterings. This is the well known Hanbury Brown-Twiss result[26] for chaotic boson fields.

However, if pionic instabilities occur that give rise to an additional source current $j_o(x)$ due to the growing collective spin-isospin waves, then a coherent component of the pion wavefunction will develop. In particular, if the only source of the pion field is $j_o(x)$, then the final pion state will be a (Glauber) coherent state:[24]

$$|j_o\rangle = e^{-\bar{n}_o/2}\ \exp\left\{i\int d^3k\ j_o(\underset{\sim}{k},\omega_k)\ a^\dagger(\underset{\sim}{k})\right\}|0\rangle \quad , \quad (52)$$

where

$$\bar{n}_o = \int d^3k\ |j_o(\underset{\sim}{k},\omega_k)|^2 \quad (53)$$

is the average number of pions radiated by $j_o(x)$. Observe that it is

crucial that $j_o(x,t)$ depend on time because only those frequency components of $j(x,t)$ with $\omega > m_\pi$ can produce on-shell pions. Also we note that for charged pions the coherent state also involves the nuclear charges in order to form eigenstates of charge. See Ref. 25 for a specific dynamic model producing charge-constrained coherent states. The remarkable property of coherent states is the absence of correlations between pions. Thus, if $j_o(x)$ were the only source of pions, then $R = 1$ for all k_1, k_2 in contrast to the results for chaotic fields.

For the general case when the source current involves both coherent and chaotic mechanisms, $j(x) = j_o(x) + j_{ch}(x)$, the pion field as only partially coherent. The correlation function is then given by[24]

$$\begin{aligned} R(\underset{\sim}{k}_1,\underset{\sim}{k}_2) &= 1 + (1-D(\underset{\sim}{k}_1))(1-D(\underset{\sim}{k}_2))\ |\rho(k_1-k_2)|^2 \\ &+ 2[D(\underset{\sim}{k}_1)D(\underset{\sim}{k}_2)\ (1-D(\underset{\sim}{k}_1))(1-D(\underset{\sim}{k}_2))]^{\frac{1}{2}}\ \rho(k_1-k_2) \quad , \end{aligned} \tag{54}$$

where $D(\underset{\sim}{k})$ is the degree of coherence of the pion field in mode $\underset{\sim}{k}$,

$$D(\underset{\sim}{k}) = \frac{|j_o(\underset{\sim}{k},\omega_k)|^2}{|j_o(\underset{\sim}{k},\omega_k)|^2 + N|j_\Delta(\underset{\sim}{k},\omega_k)|^2} \quad . \tag{55}$$

$D(\underset{\sim}{k})$ is simply the fraction of pions at $\underset{\sim}{k}$ produced by the coherent source, $j_o(x)$. Equation (54) is illustrated in Fig. 9 for the partially coherent and chaotic ($D = 0$) cases.

The important point to note is that the degree of coherence can be determined by looking at the $k_1 = k_2$ intercept point: $D(\underset{\sim}{k}) = (1-R(\underset{\sim}{k},\underset{\sim}{k}))^{\frac{1}{2}}$. Coulomb final state interactions modify these results, but before dicussing these we will construct a simple model of $j_o(x)$ to illustrate

the basic physics.

Consider a finite frequency ω_c instability in mode $\underset{\sim}{k}_c$ that grows at a rate γ. Then for small times $j_o(x,t) \sim \gamma t \exp[-i\omega_c t + i\underset{\sim}{k}_c \cdot \underset{\sim}{x}]$. To include finite size effects we modulate this form with $\exp(-x^2/2R^2)$. To take into account finite collision time $T = 1/\Gamma_T$, we modulate j_o by $\exp[-\Gamma_T t]$. We also assume that the maximum possible amplitude of the spin-isospin oscillation is the baryon density ρ. We will therefore study the simple model,

$$j_o(\underset{\sim}{x},t) = g_\pi k_c \rho \, e^{-i(\omega_c t - \underset{\sim}{k}_c \underset{\sim}{x})} \, e^{-x^2/2R^2} \, e^{-\Gamma_T t} (1 - e^{-\gamma t}) \, \theta(t) \; . \tag{56}$$

If A is the total baryon number, then ρ is related to R in this model as as $\rho = A/(2\pi R^2)^{3/2}$. Note that $g_\pi k_c$ comes from Eq. (47). With Eq. (56) we find

$$|j_o(\underset{\sim}{k},\omega_k)|^2 = A^2 \frac{g_\pi^2 k_c^2}{2\omega_k (2\pi)^3} \frac{e^{-(\underset{\sim}{k} - \underset{\sim}{k}_c)^2 R^2}}{(\omega_k - \omega_c)^2 + \Gamma_T^2} \frac{\gamma^2}{(\omega_k - \omega_c)^2 + (\gamma + \Gamma_T)^2} \; , \tag{57}$$

and the average number of coherent pions per baryon from Eq. (53) is

$$\frac{\bar{n}_c}{A} \approx \frac{g_\pi^2 k_c^2}{4\sqrt{2}\,\omega_{kc}} \rho \frac{1}{(\omega_{kc} - \omega_c)^2 + \Gamma_T^2} \frac{\gamma^2}{(\omega_{kc} - \omega_c)^2 + (\gamma + \Gamma_T)^2} \; . \tag{58}$$

That j_o produces pions coherently can be seen from Eq. (57) via the A^2 dependence of the single inclusive distribution. The coherent contribution to the single inclusive cross section therefore goes as $A^{2+2/3} = A^{8/3}$. Furthermore, the momentum distribution of coherent pions is centered on

the instability wavenumber k_c with a width ~1/R.

As a numerical example, consider $g_\pi = 1/m_\pi$, $k_c = 2m_\pi$, $\omega_{kc} = 2.24\ m_\pi$, $\rho = 2\rho_o = m_\pi^3$, $\Gamma_T = 0.2\ m_\pi$. Then

$$\frac{\bar{n}_c}{A} \approx 0.01 \left(\frac{\gamma}{m_\pi}\right)^2 \frac{1}{(1-0.45(\omega_c/m_\pi))^4} \quad . \tag{59}$$

For the condensate instability with $\omega_c = 0$, $\gamma \approx 0.2\ m_\pi$, $\bar{n}_o/A \approx 4\times 10^{-4}$. For the quasi-free pion instability, $\omega_c \approx m_\pi$, $\gamma \approx 0.2\ m_\pi$, $\bar{n}_{\pi'}/A \approx 4\times 10^{-3}$. These numbers should be compared to the observed[27] average number of π^- in Ar+Ar for lab kinetic energy E_L per nucleon, where $(\bar{n}/A)_{exp} \approx 4\times 10^{-2}(E_L/\mathrm{GeV})$. Thus, the chance of seeing coherent pion fields is best at energies $\lesssim$300 MeV/nucleon, i.e., in the sub-threshold region. Furthermore, the pion condensate instability with $\omega = 0$ would lead to far too few pions to be observable. Only the finite frequency quasi-free pion instabilities have some chance of being detectable.

The momenta, $\underset{\sim}{k}_c$, corresponding to quasi-free pion instabilities have been studied in Ref. 19. In contrast to the condensate instability which always occurs for $k_c \approx 2\text{-}3m_\pi$ and $\theta_c \approx 70°\text{-}90°$, the finite frequency instabilities occur for $k_c \approx (2\text{-}3)m_\pi$ but in an angular region that varies with energy $(\theta_1,\theta_2) \approx (0,25), (0,50), (30,60), (50,70)$ for E_L = 167, 375, 670, 1040 MeV/A. In this respect pions from the quasi-free pion instability are analogous to Cherenkov radiation.

We now discuss the current experiments on pion interferometry. Since the pioneering experiment of Ref. 28, a new high statistics experiment[29] has been performed for Ar+KCl at 1.8 GeV/nucleon. The very *preliminary* results are shown in Fig. 10.

First, we note that only the pions emerging at center of mass angles ~90° with momenta $(k)_{cm} \gtrsim 100$ MeV/c were measured in this experiment. Thus, this experiment concentrates on the pion modes, $\underset{\sim}{k}$, that are perpendicular to the beam axis. In accordance with our previous discussion, any coherence in these modes would be due to a condensate instability.

For momentum differences (in the projectile frame) $|\underset{\sim}{q}| \gtrsim 25$ MeV/c, R(q) has a shape similar to what we would expect for a completely chaotic field from a source distribution, $\rho(q)$, with radius ~5 fm. The solid curve $R(\underset{\sim}{q})$ corresponds to a shell of radius r = 5 fm. For $|\underset{\sim}{q}| < 25$ MeV/c we see, however, an anti-correlation effect. This hole is, however, due mostly to final state Coulomb interactions between the $\pi^-\pi^-$ pair. This Coulomb interaction leads to a modulation[24] of R(q) by a (Gamow) penetration factor, $G(q) = 2\pi\eta(\exp(2\pi\eta) - 1)^{-1}$, $\eta = \alpha m_\pi/q$. There is qualitative agreement between the dashed curve including this G(q) and the hole in the data. However, because of the very preliminary nature of the data, no conclusion can be drawn at this time from the possible excess suppression at low $|\underset{\sim}{q}|$. What Fig. 10 is supposed to convey is that high precision pion interferometry experiments are possible and that it will be possible to place upper bounds on the degree of coherence for these perpendicular modes in the near future.

We close this discussion by pointing out again that to search for coherence associated with possible finite frequency, quasi-free pion modes, future experiments should concentrate on pion modes in the forward and mid θ_{cm} directions as well. As we saw in Eq. (59), many more pions would be produced from finite frequency instabilities than the condensate instability. Furthermore, these coherent components would be more easily

seen at lower energies, 100-300 MeV/nucleon, below the threshold for the chaotic component.

IV. OUTLOOK

In Section II, we showed first how correlations, Δ production, and form factors can be included in a mean field theory by a nearly density independent renormalization of the πNN coupling. Second, we showed how the constraints of bulk nuclear properties can be incorporated in a relativistic mean theory developed in Ref. 2. These constraints greatly restrict the condensate energy as we saw in Fig. 3. Nevertheless, the sizable spin-isospin oscillations (Fig. 6) are rather insensitive to model details. In Section III, we explored how these growing collective spin-isospin waves could affect the dynamics in nuclear collisions. First critical scattering was discussed, then the complications of searching for direct evidence for this phenomena via large-angle proton correlations were discussed. Second, the use of pion interferometry to look for coherent pion field was discussed. A simple calculation of the number of coherent pions was presented from which we concluded that rather few pions could be created coherently. Finally, we emphasized that coherence in the finite frequency modes is more likely to be observable than in the condensate mode. Unfortunately, even these modes lead to only a small number of pions. It remains to be seen whether future experiments can develop the sophistication necessary to look for such subtle coherent pion phenomena amidst the complex background due to incoherent intranuclear cascading.

Although not discussed in this report, we also note the search for precritical pion phenomena via (e,e') and (p,p') reactions (see,Ref.30).

ACKNOWLEDGMENTS

Very profitable discussions with N. K. Glendenning during the course of this report is gratefully acknowledged, especially during the preparation and presentation of preliminary unpublished results, Fig. 2-6 of Ref. 2. I am also grateful to W. Zajc and K. Crowe for permission to present their preliminary results,[29] Fig. 10, and to S. Nagamiya and I. Tanihata for discussions about their experiment,[22,23] Fig. 8.

This work was supported by the Office of Nuclear Physics of the U.S. Department of Energy under contract W-7405-ENG-48.

APPENDIX A: $\langle\pi\rangle \to 0$ Limit of MFA

Here we want to derive the connection between the propagator and MFA approaches. Such a connection was discussed by Baym in his Les Houch lectures.[1] We present an alternate and more explicit derivation here.

We start from the pion mean field equation, Eq. (19c),

$$(\Box + m^2)\, \langle \underset{\sim}{\pi}(x)\rangle = \underset{\sim}{J}_\pi(x) \tag{A.1}$$

where

$$\underset{\sim}{J}_\pi(x) = g_\pi\, \partial^\mu \langle \bar{\psi}(x)\gamma_5\gamma_\mu \underset{\sim}{\tau}\psi(x)\rangle \quad , \tag{A.2}$$

which depends implicitly on $\langle\underset{\sim}{\pi}(x)\rangle$. In terms of the full propagator $S_\pi(x,y)$, which satisfies Eq. (19d) with $\delta^4(x-y)$ replacing 0 on the right-hand side, we can write as in Eq. (25),

$$\underset{\sim}{J}_\pi(x) = -ig_\pi\, \partial^\mu\, \mathrm{Tr}\,\{\gamma_5\gamma_\mu \underset{\sim}{\tau}\, S_\pi(x,x^+)\} \tag{A.3}$$

where $x^+ = (\underset{\sim}{x}, t+0)$. We now expand $J_\pi(x)$ to first order in $\langle\underset{\sim}{\pi}(y)\rangle$:

$$\underset{\sim}{J}_\pi(x) = \underset{\sim}{J}_0(x) + \int d^4y \left[\frac{\delta \underset{\sim}{J}_\pi(x)}{\delta\langle\underset{\sim}{\pi}(y)\rangle}\right]_{\langle\pi\rangle\to 0} \langle\underset{\sim}{\pi}(y)\rangle + 0(\langle\pi\rangle^2) \ . \tag{A.4}$$

Defining

$$\Pi_{ij}(x,y) = -\lim_{\langle\underset{\sim}{\pi}(y)\rangle\to 0} \left\{\frac{\delta\, J^i_\pi(x)}{\delta\langle\pi_j(y)\rangle}\right\} \ , \tag{A.5}$$

and noting that the divergence of the axial current is zero when

$\langle \underset{\sim}{\pi} \rangle = 0$ ($\underset{\sim}{J}_o = 0$), we can rewrite Eq. (A.1) to first order in $\langle \underset{\sim}{\pi}(x) \rangle$ as

$$(\Box + m_\pi^2) \langle \pi_i(x) \rangle = -\int d^4y \, \Pi_{ij}(x,y) \langle \pi_j(y) \rangle \quad . \tag{A.6}$$

In symmetric homogeneous nuclear matter $\Pi_{ij}(x,y) = \delta_{ij} \Pi(x-y)$, and

$$(\Box + m_\pi^2) \langle \pi_i(x) \rangle = -\int d^4y \, \Pi(x-y) \langle \pi_i(y) \rangle \quad . \tag{A.7}$$

Expanding $\langle \pi_i(x) \rangle$ in Fourier components, we get finally

$$(-k^2 + m_\pi^2) \, \pi_i(k) = -\Pi(k) \, \pi_i(k) \quad . \tag{A.8}$$

Taking, however, the Fourier transform of Eq. (A.1) shows that the right-hand side is just $J_i(k)$. Therefore,

$$\Pi(k) = - \lim_{\pi_i(k) \to 0} \left\{ \frac{J_i(k)}{\pi_i(k)} \right\} \quad . \tag{A.9}$$

In order to compute $\Pi_{ij}(x,y)$ or $\Pi(k)$ explicitly from Eq. (A.5), we can start from the integral equation for $S_\pi(x,y)$:

$$S_\pi(x,y) = S_o(x,y) + \int d^4z \, S_o(x,z) \, g_\pi \, \gamma_5 \gamma^\mu \frac{\partial}{\partial z^\mu} \langle \pi_i(z) \rangle \, \tau_i S_\pi(z,y) \quad . \tag{A.10}$$

where $S_o(x,y)$ is the nucleon propagator when $\langle \pi \rangle = 0$. First integrate by parts to transfer the $\partial/\partial z^\mu$ away from the π field. Then recall that

$$\frac{\delta \langle \pi_i(x) \rangle}{\delta \langle \pi_j(y) \rangle} = \delta_{ij} \, \delta^4(x-y) \quad . \tag{A.11}$$

Thus,

$$\lim_{\langle\pi_j(y)\rangle\to 0} \frac{\delta S_\pi(x,z)}{\delta\langle\pi_j(y)\rangle} = -\frac{\partial}{\partial y^\nu}\left\{S_o(x,y)\; g_\pi \gamma_5\gamma^\mu \tau_j S_o(y,z)\right\} . \tag{A.12}$$

Using Eqs. (A.3) and (A.5), we obtain finally,

$$\Pi_{ij}(x,y) = -ig_\pi^2 \frac{\partial}{\partial x^\mu}\frac{\partial}{\partial y^\nu} \mathrm{Tr}\left(\gamma_5\gamma^\mu \tau_i S_o(x,y)\; \gamma_5\gamma^\nu \tau_j S_o(y,x)\right) , \tag{A.13}$$

and therefore in symmetric homogeneous nuclear matter,

$$\Pi(k) = -2ig_\pi^2 \int \frac{d^4p}{(2\pi)^4} \mathrm{Tr}\left(\gamma_5 \not{k} S_o(p)\; \gamma_5 \not{k} S_o(p+k)\right) . \tag{A.14}$$

In the non-relativistic limit ($p_F \ll m^*$),
$S_o(p) \to (2m^*)^{-1}(p_o - g_v V_o - p^2/2m^* + i\varepsilon\, \theta(p_F - p))^{-1}$, Trace $\to -8|\underset{\sim}{k}|^2$ and
$\Pi(k)$ reduces to the familiar Lindhard function (see, e.g., Ref. 7).

REFERENCES

1. For extensive review, see A.B.Migdal; Rev. Mod. Phys. 50 (1978) 107; W.Weise and G.E.Brown; Phys. Reports 27C (1976) 1; T.D.Lee; Rev. Mod. Phys. 47 (1975) 267; G.Baym; Les Houches 1977, Session XXX, Vol. 2, p.748; also D.K.Campbell, R.F.Sawyer, H.Pirner in same Les Houches Lectures.
2. B.Banerjee, N.K.Glendenning, M.Gyulassy; preprint LBL-10572 (April 1980), and to be published.
3. K.Johnson, Acta Physica Polinica B6 (1975) 865.
4. G.E.Brown, M.Rho; Phys. Lett. 82B (1979) 177.
5. S.Theberge, A.W.Thomas, G.A.Miller; to be published.
6. J.W.Clark, Washington University thesis (1979).
7. M.Gyulassy, W.Greiner; Ann. Phys. 109 (1977) 485.
8. W.Weise, G.E.Brown; Phys. Lett. 58B (1975) 300.
9. Y.Futami, H.Toki, W.Weise; Phys. Lett. 77B (1978) 37.
10. V.Ruck, M.Gyulassy, W.Greiner; Z. Phys. A277 (1976) 391.
11. K.K.Gudima, V.D.Toneev; Dubna JINR preprint E2-12624 (1979).
12. G.G.Bunatjan; Yad. Fiz. 29 (1979) 258 [Sov. J. of Nucl. Phys. 30 (1979) 131].
13. H.J.Pirner, K.Yazaki, P.Bonche, M.Rho; Nucl. Phys. A329 (1979) 491.
14. J.D.Walecka; Ann. Phys. 83 (1974) 491.
15. S.A.Chin; Ann. Phys. 108 (1977) 301.
16. A.K.Kerman, L.D.Miller; Proceedings of 2nd High Energy Heavy Ion Summer Study, LBL-3675 (1974), p.73.
17. J.Boguta, A.R.Bodmer; Nucl. Phys. A292 (1977) 413.

18. W.H.Dickhoff, A.Faessler, J.Meyer-ter-Vehn, H.Mather; Phys. Rev. C, to be published.

19. M.Gyulassy; LBL-6525, in Proceedings of the Falls Creek Falls Meeting on Heavy Ion Collisions, June 13-17, 1977.

20. J.Knoll, J.Randrup; Nucl. Phys. A324 (1979) 445; J.Knoll; to be published.

21. P.Hecking, H.Pirner; Nucl. Phys. A333 (1980) 514.

22. S.Nagamiya, et al.; Phys. Lett. 81B (1979) 147.

23. I.Tanihata, et al.; preprint LBL-10694 (1980).

24. M.Gyulassy, S.K.Kauffmann, L.W.Wilson; Phys. Rev. C20 (1979) 2267.

25. S.K.Kauffmann, M.Gyulassy; Nucl. Phys. A333 (1980) 392.

26. F.B.Yano, S.E.Koonin; Phys. Lett. 78B (1978) 556.

27. L.Schroeder, A.Sandoval; private communication.

28. S.Y.Fung, et al.; Phys. Rev. Lett. 40 (1978) 292.

29. W.Zajc, J.Bistirlich, R.Bossingham, H.Bowman, C.Clawson, K.Crowe, J.Ingersoll, M.Koike, C.Martoff, J.Miller, J.Rasmussen, J.Sullivan, P.Truol; Bull. Am. Phys. Soc. (April 21, 1980), to be published.

30. H.Toki, Proceedings of the RCNP-Kikuchi Summer School, Osaka, Japan, May, 19-23, 1980, Univ. Regensburg preprint.

FIGURE CAPTIONS

Fig. 1. Phase diagram for pion condensation prepared by Gudima and Toneev.[11] Curves RGG (Ref. 10) and B (Ref. 12) are calculated critical temperatures illustrating sensitivity of $T_c(\rho)$ to model assumptions. The dynamical paths via nuclear cascade calculations[11] for two nuclear collisions are also indicated along with the time in 10^{-23} sec.

Fig. 2. Binding energy per nucleon in MFA of Ref. 2. Parameters are $g_s/m_s = 15/m_N$, $g_v/m_v = 11/m_N$, $b = 0.004$, $c = 0.008$, $m_N = 4.77$ fm^{-1}, $|\underset{\sim}{k}| = 1.5$ fm^{-1}. The $\pi_c = 0$ solution is the non-condensed equation of state. Self-consistent condensate solutions exist for $g_\pi > 1.18$ fm. Two examples are shown.

Fig. 3. Same as Fig. 2 but $g_s/m_s = 6/m_N$, $g_v/m_v = 4.7/m_N$, $b = -0.734$, $c = 6.86$ giving larger m^*/m_N. In contrast to Fig. 2, condensate solutions exist also for $g_\pi \approx 1$ fm (see Table 1).

Fig. 4. The effective mass[2] for Fig. 2 (stiffer) and Fig. 3 (softer) compared to Walecka's model.[14]

Fig. 5. The condensation energy from Fig. (3), $g_\pi = 1$ fm, compared to chiral model result.[13] Dashed curve illustrates unrenormalized $g_\pi = 1.41$ fm case in Fig. 3.

Fig. 6. (a) The amplitude R_{53} of the spin-isospin oscillation measured in units of the baryon density for $g_\pi = 1$ fm case of Fig. 3. Also indicated are the values of the pion condensate field $\bar{\pi}$

in units of m_π. The condensation energy is also reproduced from Fig. 5.

(b) Illustration of the magnitude of oscillation of the proton, spin up (P↑), neutron spin down (N↓), etc., densities for $R_{53} = 0.5$ as a function of the coordinate parallel to the condensate momentum.

Fig. 7. Example of critical scattering associated with pionic instabilities from Ref. 7. Dashed curve is model of free space elastic cross section and $d\sigma_{eff}$ is the result of polarization effects, Eq. (40). In (b) the polarization factor P(0,k) is plotted vs. the momentum transfer k.

Fig. 8. Two proton correlation data of Refs. 22,23. Contours are the in-to-out-of plane correlation function, Eq. (46). Shaded area is acceptance of one tag counter. The peak is associated with quasi-elastic scattering component.

Fig. 9. Ideal pion interferometry correlation function, Eq. (54), for partially coherent fields.[24] $D(\underset{\sim}{k}) = 0$ case is the usual chaotic field result. Coulomb distortions are not included.

Fig. 10. Preliminary data[29] for $R(\underset{\sim}{k}+\underset{\sim}{q}/2, \underset{\sim}{k}-\underset{\sim}{q}/2) = R(\underset{\sim}{q})$ for pion modes $\underset{\sim}{k}$ perpendicular to the beam axis in the center of mass, plotted as a function of the momentum difference $|\underset{\sim}{q}|$ (in the projectile frame). Solid curve is expected R for chaotic fields from an R = 5 fm source. Dashed curve includes Gamow Coulomb correction factor.

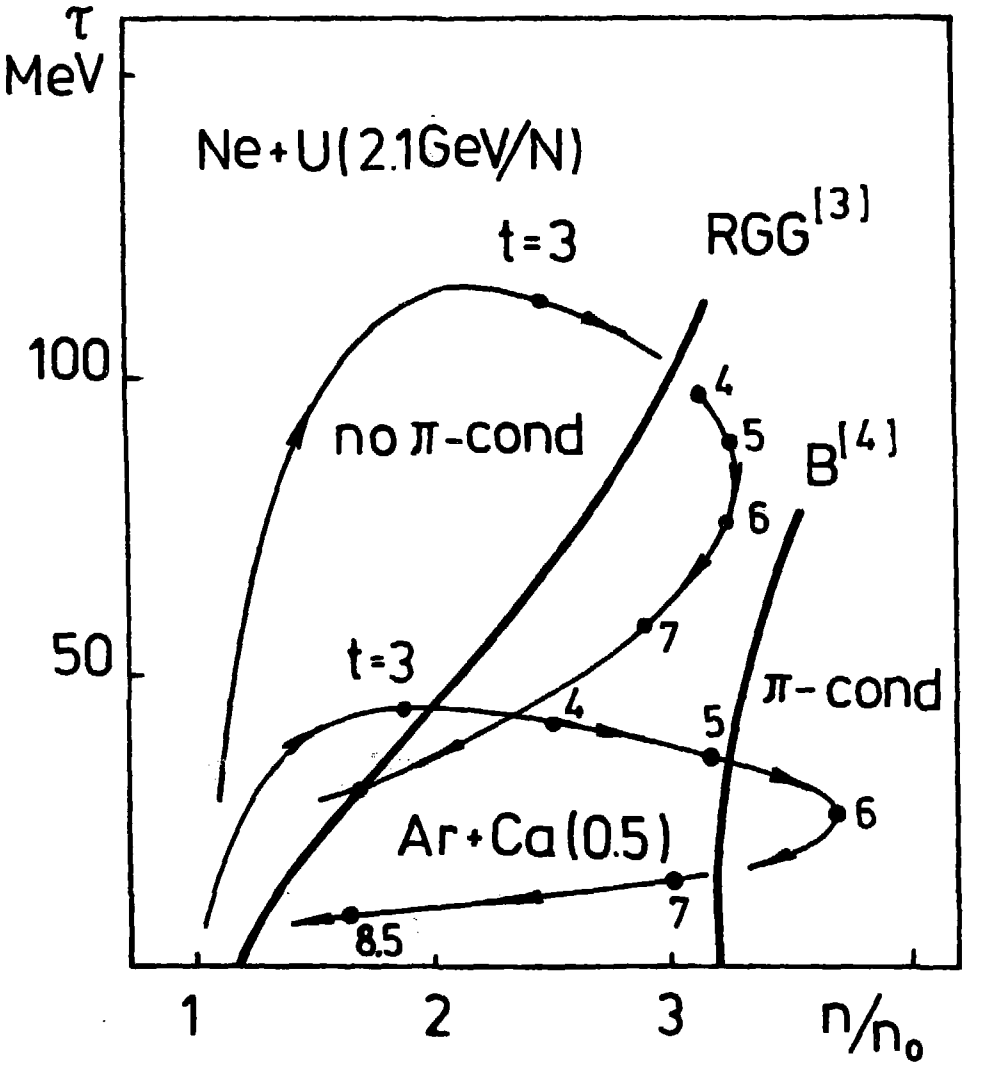

XBL 805-9738

Fig. 1

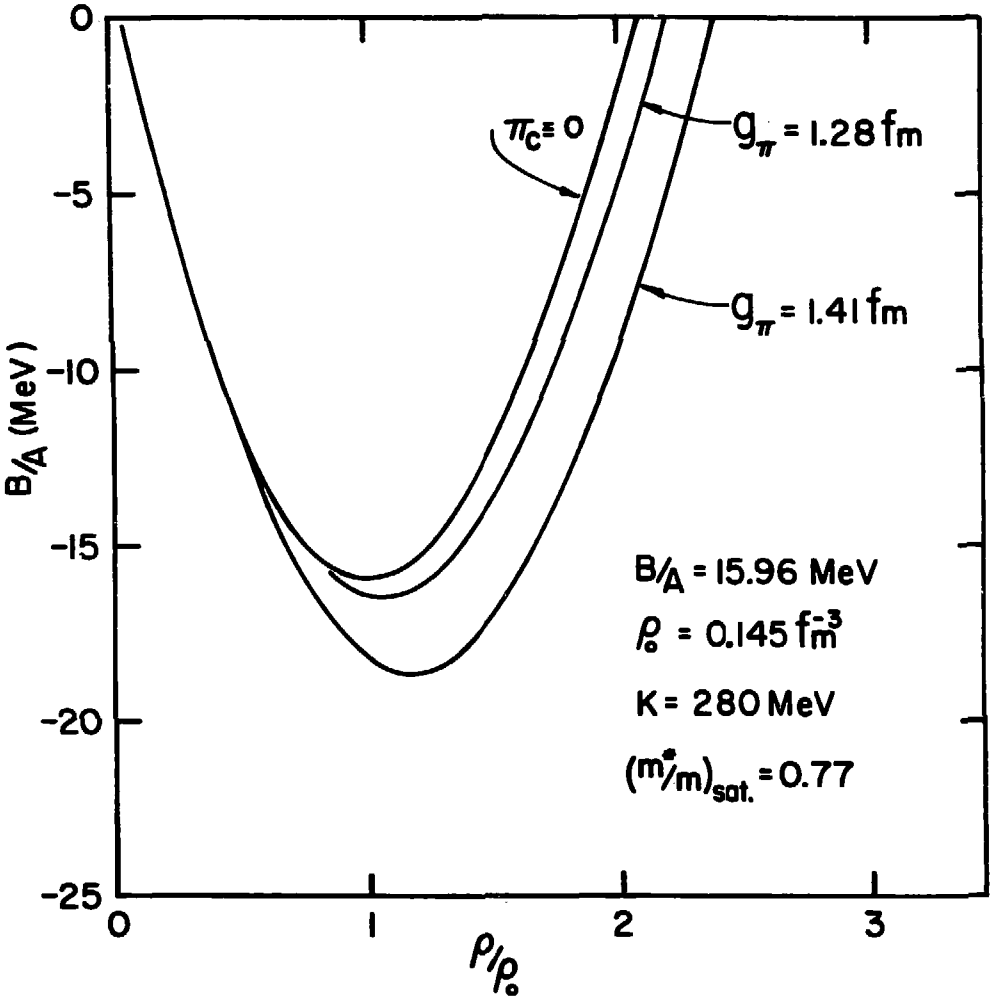

XBL 7912-5246

Fig. 2

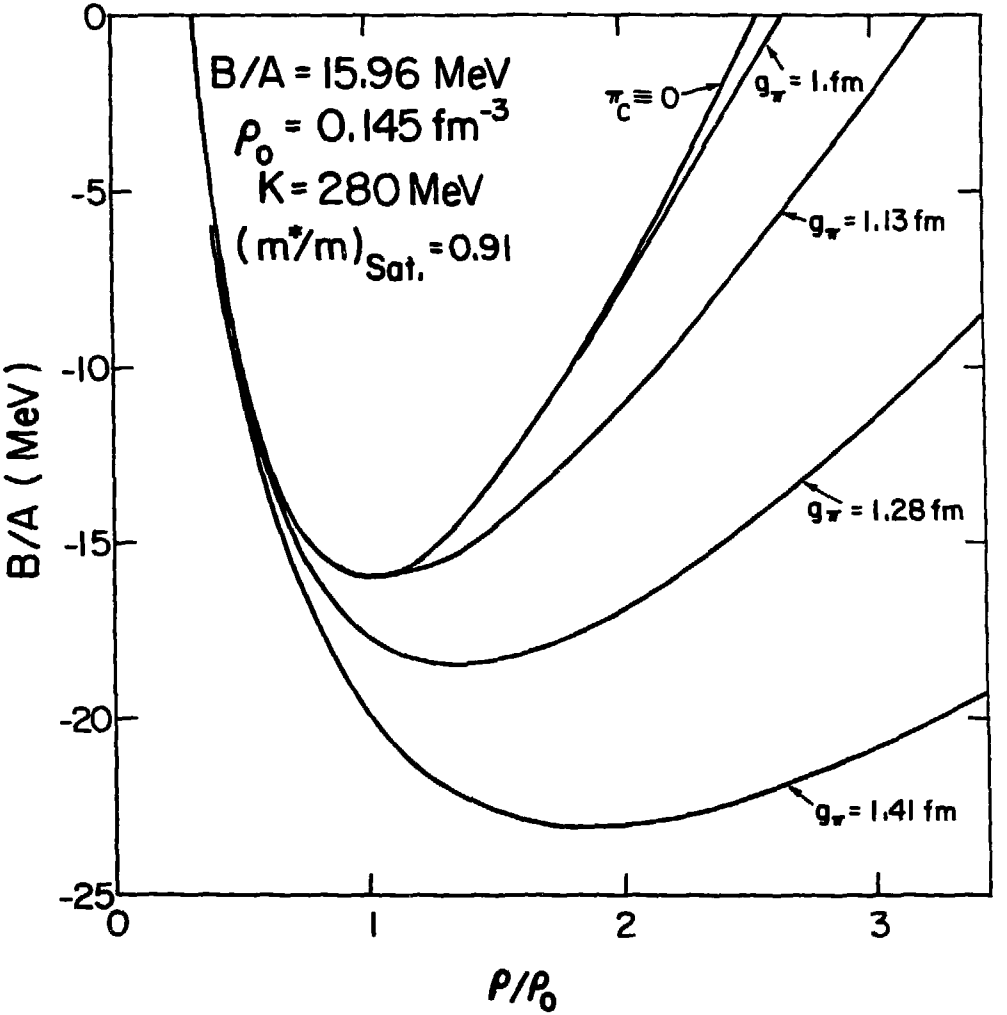

XBL 805-837

Fig. 3

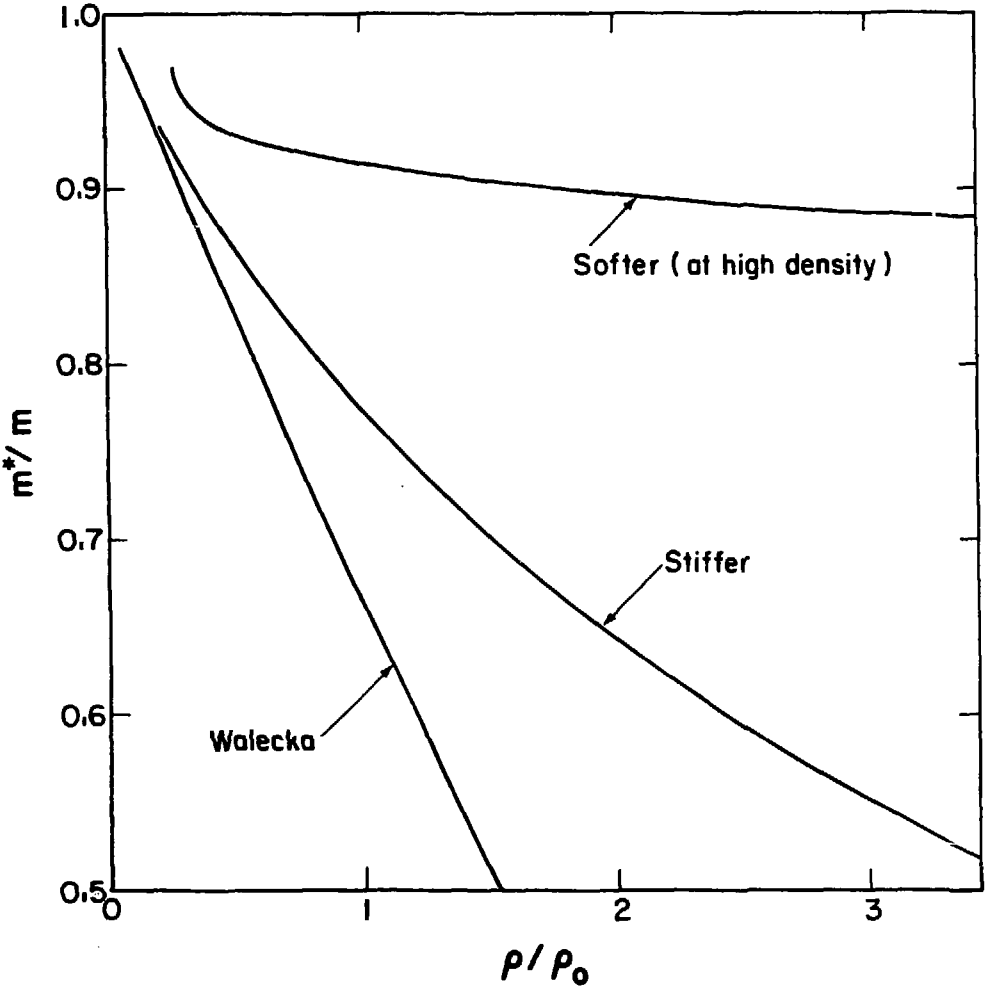

XBL 805-835

Fig. 4

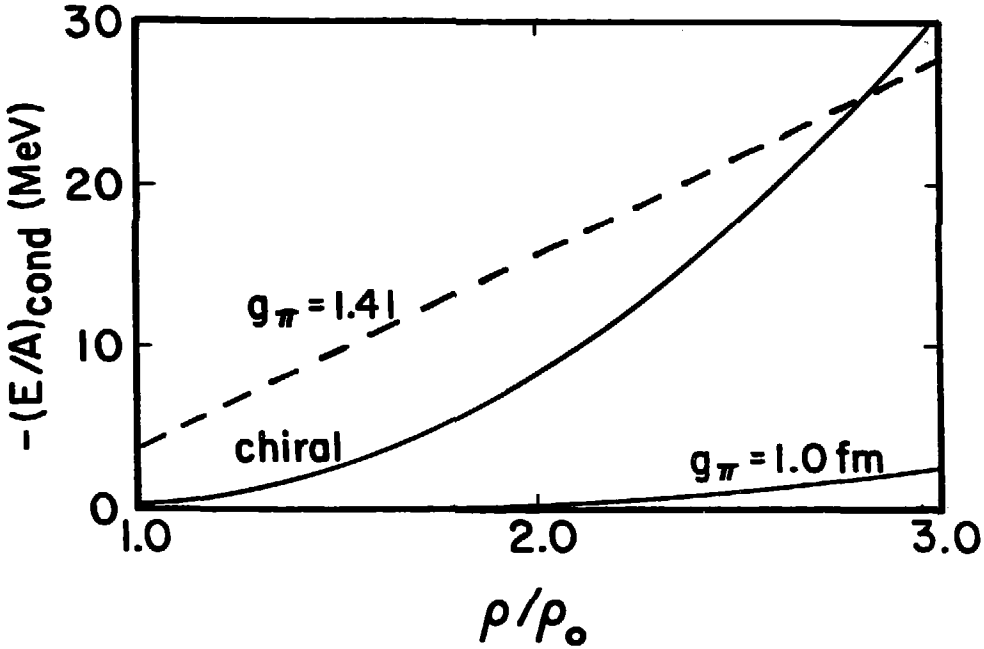

XBL 805-9728

Fig. 5

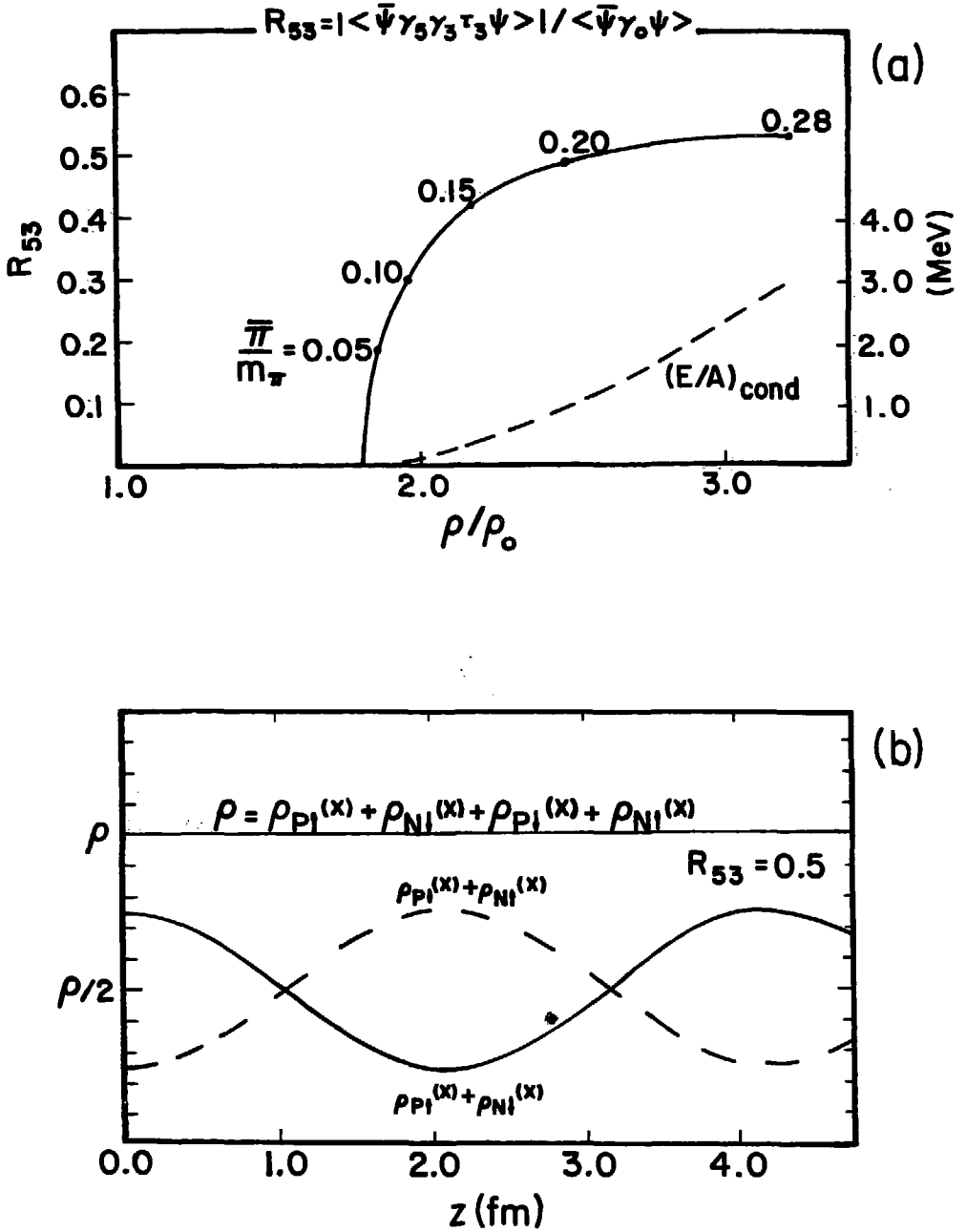

XBL 805-9726

Fig. 6

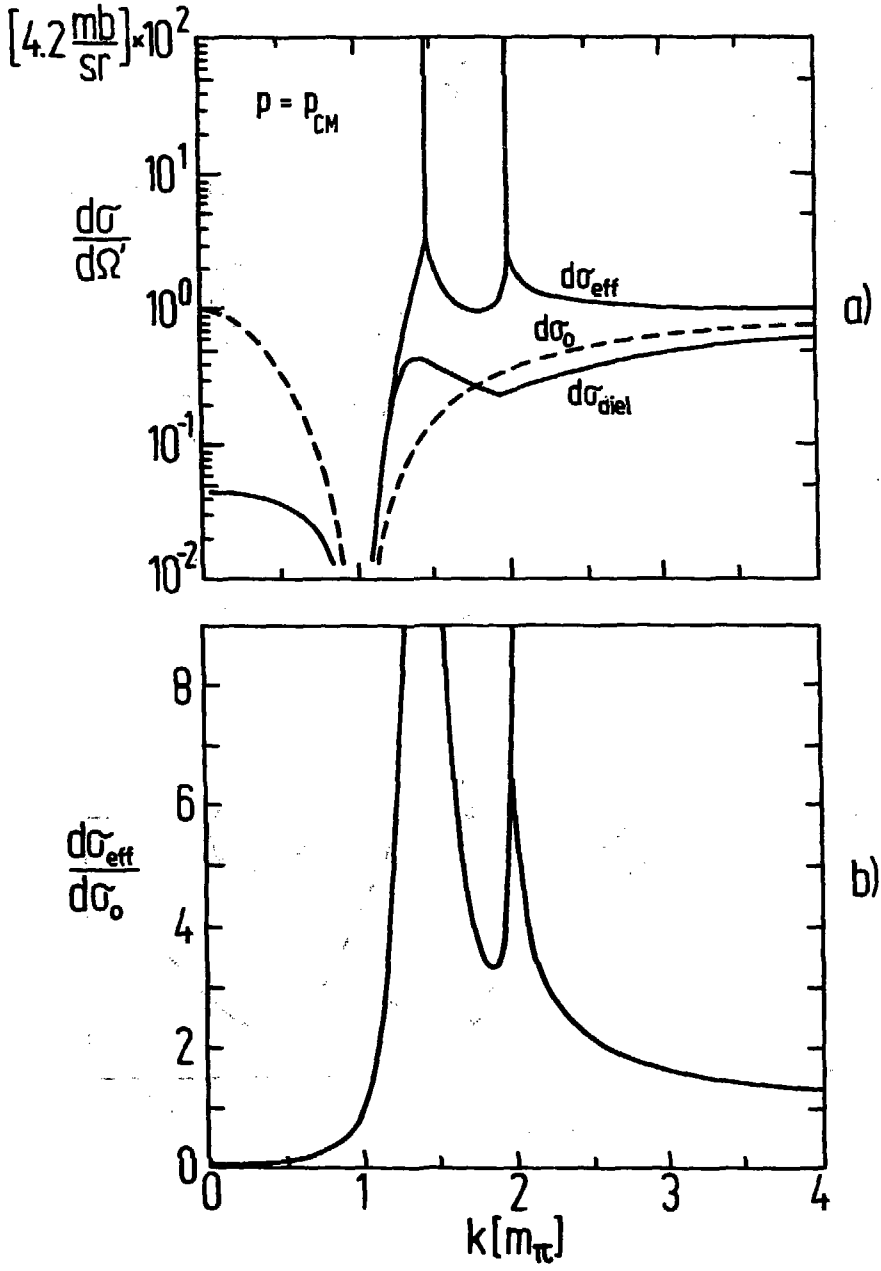

XBL 772-7475

Fig. 7

firestreak[27] and cascade[52] models. However, the predicted slopes are larger than those observed. For a given Q, it is found that the square of the dispersion is equal to the mean number of negative pions. This is shown in Fig. 35(c). This result has also been reported by Bartke[48] for ^{12}C central collisions studied at Dubna. These dispersions for the negative pion multiplicities are dominated by fluctuations in pion production and absorption rather than the dispersion associated with elementary N-N pion production processes at these energies.

Figure 36 shows the energy dependence for central collisions of the average negative pion multiplicity in the c.m. frame. A linear dependence of $\langle n_{\pi^-} \rangle$ is observed above 150 MeV/nucleon with a slope of $0.02\pi^-$/(MeV/nucleon). The low energy point falls off this trend, presumably due to effects of Fermi motion which are very important near threshold. Thermal models are not able to reproduce this result, and consistently overestimate pion yields by a factor of 2 or more. A Fermi gas model[53] which assumes thermal but no chemical equilibrium between N's, Δ's, π's, ρ's; is able to reproduce this trend (except near the upper end). To do this, it assumes zero impact parameter and uses the isobar model pion ratios to predict the numbers of negative pions. Absorption effects, including the process, $\Delta + N \rightarrow NN$, are known to reduce the pion yields by as much as 30-50 percent at these energies. Another way of looking at the trend with energy is shown in Fig. 37, where the multiplicity distributions for negative pions for a central trigger are shown for each of the ^{40}Ar energies. Once the bombarding energy is well above the pion threshold, these distributions are approximately Gaussian in shape.

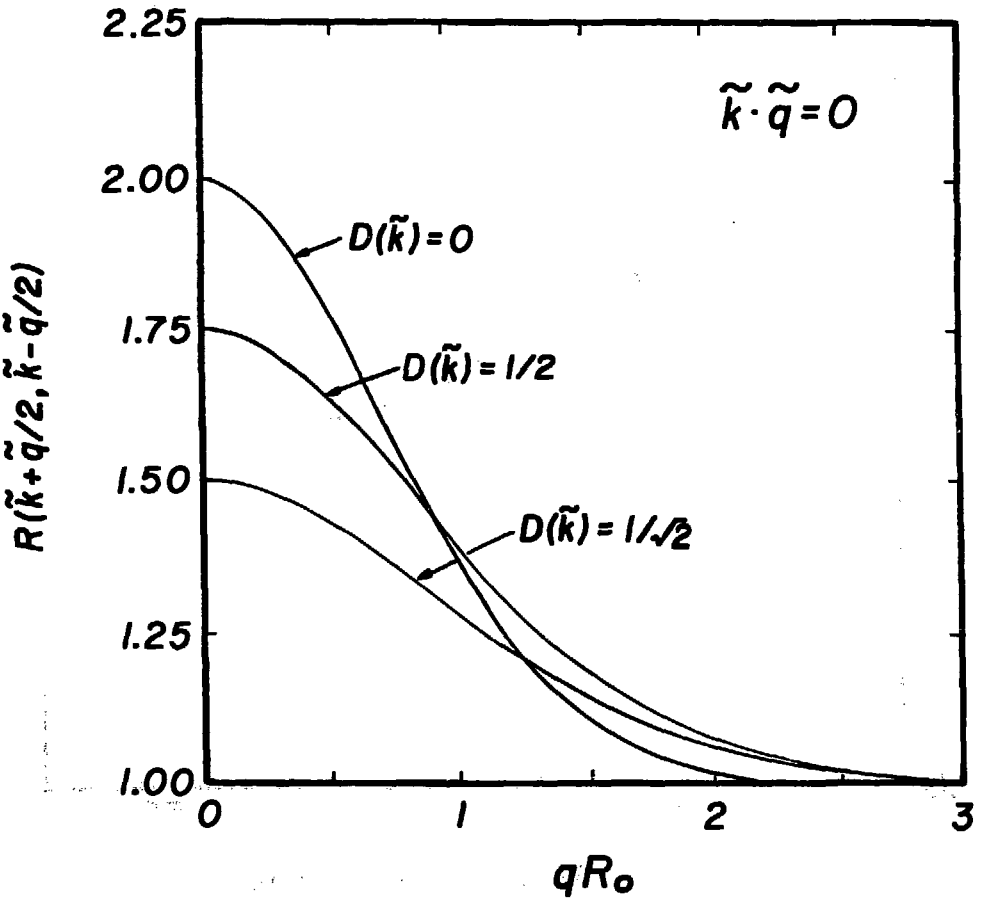

XBL 793-8709

Fig. 9

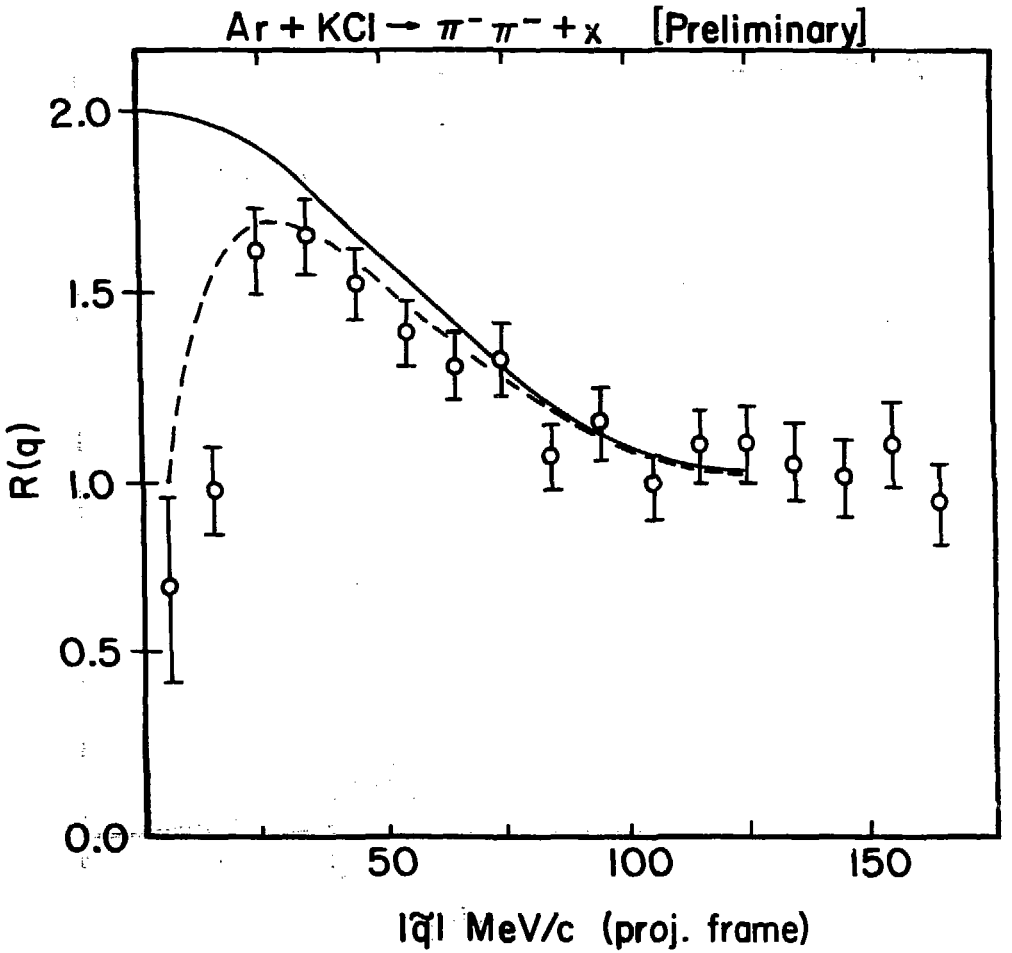

XBL 805-9727

Fig. 10